Constant Proportion Portfolio Insurance Strategies in Contagious Markets *

Alice Buccioli† and Thomas Kokholm‡

Department of Economics and Business Economics
Aarhus University
Fuglesangs Allé 4
8210 Aarhus V
Denmark

July 25, 2017

Abstract

Constant Proportion Portfolio Insurance (CPPI) strategies are popular as they allow to gear up the upside potential of a stock index while limiting its downside risk. From the issuer's perspective it is important to adequately assess the risks associated with the CPPI, both for correct "gap" fee charging and for risk management. The literature on CPPI modeling typically assumes diffusive or Lévy-driven dynamics for the risky asset underlying the strategy. In either case the self-contagious nature of asset prices is not taken into account. In order to account for contagion while preserving analytical tractability, we introduce self-exciting jumps in the underlying dynamics via Hawkes processes. Within this framework we derive the loss probability when trading is performed continuously. Moreover, we estimate measures of the risk involved in the practical implementation of discrete-time rebalancing rules governing the CPPI product. When rebalancing is performed on a frequency less than weekly, failing to take contagion into account will significantly underestimate the risks of the CPPI. Finally, in order to mimic a situation with low liquidity, we impose a daily trading cap on the risky asset and find that the Hawkes process driven models give rise to the highest risk measures even under daily rebalancing.

KEYWORDS: CPPI, self-contagion, Hawkes processes, gap risk, liquidity, risk measures.

---

*The authors acknowledge Andrea Barletta, Elisa Nicolato, and Rolf Poulsen for useful comments. The paper has been presented at the 9th World Congress of the Bachelier Finance Society, New York, at VCMF 2016, Vienna, and at the 21st International Congress on Insurance: Mathematics and Economics, Vienna. Wharton Research Data Services (WRDS) was used in preparing this manuscript. This service and the data available thereon constitute valuable intellectual property and trade secrets of WRDS and/or its third-party suppliers.

†abuccioli@econ.au.dk

‡thko@econ.au.dk

Contents

1 INTRODUCTION

We study the risk embedded in the Constant Proportion Portfolio Insurance (CPPI) trading strategy in a jump-diffusion model where the price of the underlying asset may experience self-contagion. CPPI strategies are popular dynamic portfolio strategies that allow investors to gear up the upside potential while limiting the downside risk. This contrasts the more straightforward insurance strategy involving static positions in a risky asset and a put option, where the upside participation is non-geared. Especially, many pension companies are turning to CPPI strategies in order to honor return guarantees embedded in many retirement plans, as traditional investments in government bonds do not offer sufficient returns in the current low interest rate environment. In an ideal world, the CPPI strategy puts a limit to the portfolio loss while allowing for unlimited upside. The investor will profit from the upward potential of a risky asset while having a guaranteed fixed amount of capital G at the maturity of the CPPI. This is achieved by investing dynamically in a "riskfree" asset, typically a bond, and a risky asset, typically comprised of a stock index. Let B_t denote the *bond floor* representing the minimal wealth that will ensure the guarantee G at maturity. For a stylized CPPI with no funding constraints and as long as the value of the strategy $V_t \geq B_t$, the exposure e_t to the risky asset is determined as $e_t = m(V_t - B_t) = mC_t$, where $m > 0$ is a multiplier reflecting the risk-appetite of the investor and the *cushion* C_t is defined as the excess of the portfolio value over the bond price. The surplus part, that is the difference between the strategy value and the risky exposure, will be allocated into the riskfree asset. In case the portfolio value breaks the floor B_t, the remaining wealth is invested in the bond and held until maturity to prevent the risk of imperiling the capital further. The risk of breaching the floor is referred to as the *gap risk*.

In an idealized setting under continuity assumptions imposed both on the trading frequency and the dynamics of the risky asset, the risk of breaching the floor of the CPPI is zero. However, in practice both assumptions are violated: first, as the CPPI is often written on risky funds with low liquidity the rebalancing frequency of the CPPI is typically performed monthly or even quarterly (Hirsa, 2009) making the risk of breaching the floor between trading dates non-negligible. Second, it has been widely documented that price trajectories contain jumps (Ait-Sahalia and Jacod, 2009; Andersen et al., 2002; Barndorff-Nielsen and Shephard, 2006), which introduces a risk of breaching the floor even under continuous-time trading.

The first point is addressed in Balder et al. (2009) where the effectiveness of CPPI strategies under discrete-time trading is studied. They analyze a discretely rebalanced CPPI under the assumption that the risky asset evolves as a geometric Brownian motion. The second point is addressed in Cont and Tankov (2009), where they relax the continuity assumption of the price process and study the risk of the CPPI in models driven by Lévy processes and under continuous-time trading. In order to relax the time-homogeneity assumption, Weng (2013) generalizes the study of Cont and Tankov (2009) to include regime switching of the driving exponential Lévy processes, but still under the continuous-time trading assumption.

There is a risk-return trade-off between the rebalancing frequency of the trading strategy and the riskiness of the CPPI. Reducing the gap risk of the CPPI portfolio by more frequent trading will come at the cost of higher transaction costs. In a setting including stochastic volatility and time-homogeneous jumps, Jessen (2014) compares different rebalancing strategies and ranks their performance for an investor with power utility. She finds that the optimal rebalancing rule should depend both on transaction costs and the changes in the risky asset. In a related study Branger et al. (2010) find that in a setting where the risky asset is driven by a geometric Brownian motion, an individual with HARA utility and subsistence level will find the CPPI strategy optimal among different investment strategies with possible guarantees attached. Pézier and Scheller (2013) extend the analysis of Branger et al. (2010) to a more realistic setting with discrete-time rebalancing and with price trajectories that contain time-homogeneous jumps, and arrive at the same conclusion as Branger et al. (2010), namely that for HARA investors the CPPI strategies dominate trading strategies where the downside is protected via a put option.

Within this framework, we conduct a study of the gap risk coverage associated with CPPI strategies. First, under the assumption of frictionless and continuous trading, the modeling setup we propose allows for an analytical expression for the probability of breaching the floor. Second, to bring the level of our analysis closer to wealth allocations in actual CPPI issuances, we employ discrete-time trading and we investigate the risk of a CPPI portfolio attributable to both price crashes and discrete-time readjustments. In such discrete trading context, we estimate measures of the risk involved in the practical implementation of the CPPI strategy. For models calibrated to option prices, we find that the impact of contagion on the fair "gap risk fee" is of smaller magnitude. However, for risk measures corresponding to the tail of the loss distribution we find that neglecting to take the contagion into account will underestimate those measures of the CPPI significantly when the rebalancing is done at a frequency lower than weekly. Moreover, we add illiquidity to the model and impose a cap on the daily trading in the risky asset. We find that for illiquid assets the impact of contagion on tail risk measures is significant even in the case of daily rebalancing, since the CPPI might loose additional value after the floor is breached if the risky exposure can not be sold off in one block. Finally, we compare the Constant-Mix trading strategy to the CPPI in terms of risk measures and find that, for low levels of rebalancing and in distressed market conditions, the risk measures of the CPPI are higher than those of the Constant-Mix strategy, despite that the former strategy has a capital guarantee built in.

The hypothesis of self-contagion in financial markets is tested by Aït-Sahalia et al. (2015), where they provide clear evidence that "markets strongly self-excited during the recent financial crisis" and they conclude towards jump self-excitation. In our context this has the consequence that a negative shock to the risky asset underlying the strategy will lead to an increased probability of additional negative shocks occurring to the asset. Neglecting to take the contagious nature of jumps into account will underestimate the risks connected to a discretely rebalanced strategy, as the probability of realizing several "big" negative jumps to the asset over a short time-span is "small" in a traditional Lévy process driven jump model. The self-contagion effect is achieved by introducing self-exciting jumps in the underlying dynamics via Hawkes processes (Hawkes, 1971). While in Lévy-driven models the intensity of adverse shocks is constant, self-exciting jump processes account for the risk of jump clustering documented in real markets. Serving as anecdotal evidence Figure 1 depicts the log-returns of the SPX index over a period of two weeks in 2008. As shown in the figure the daily log-return falls below three standard deviations of the returns (computed based on a sample of 15 years) a total of 4 times. The probability of this occurring in a more traditional Lévy driven jump model is essentially zero. Hawkes processes have been applied for financial modeling in a number of contexts: in Errais et al. (2010); Aït-Sahalia et al. (2014); Dassios and Zhao (2011) for credit modeling, for index derivatives modeling in Kokholm (2016); Boswijk et al. (2015), to model the term structure of interest rates in Hainaut (2016), in Aït-Sahalia and Hurd (2016) to study optimal portfolio allocation in a multivariate modeling framework allowing for contagion among the risky assets, to fit extremal behaviors of financial time series in Embrechts et al. (2011), and to estimate conditional value at risk in Chavez-Demoulin et al. (2005); Herrera and Schipp (2013). In an insurance context, Stabile and Torrisi (2010) study the ruin problem in a risk model with Hawkes claims arrivals. Dassios and Zhao (2012) extend the analysis of Stabile and Torrisi (2010) by using a generalization of the Hawkes process and the Cox process to include both self-excited and externally excited jumps. In a related study Jang and Dassios (2013) further extend the study using a bivariate self-exciting process to quantify also collateral losses. With the availability of high-frequency data, considerable attention has been devoted to the modeling of market price microstructure using Hawkes processes: Bowsher (2007) proposes a joint model for transaction times and prices at high frequency, Chavez-Demoulin and McGill (2012) apply Hawkes processes based on a generalized Pareto distribution to capture extreme losses and their clustering in order to model intraday value at risk, in Bacry et al. (2013) multivariate Hawkes processes are applied to model order books at high frequency, and finally Jaisson et al. (2015) suggest that general Hawkes processes on large time scales can be considered asymptotically as Brownian motions.

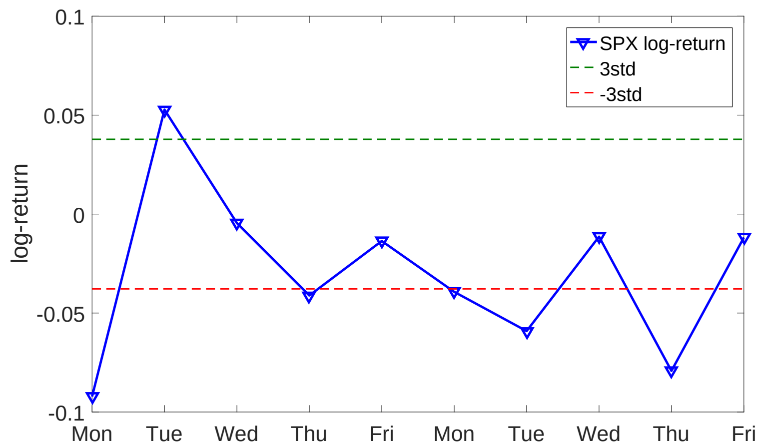

Figure 1: Log-returns of the SPX index in the period from September 29, 2008 to October 10, 2008. The indicated lines with three times the standard deviations have been calculated based on the sample from September 1, 2000 to August 31, 2015.

The rest of the article is structured as follows. In Section 2, we introduce self-exciting jump processes and specify the model setup. Section 3 presents the CPPI structure and, under a continuity assumption on the trading frequency, the probability of a loss is derived in analytic form. In Section 4 we calibrate the model to SPX option prices using Fourier transform methods. In Section 5 we conduct a simulation study of the gap risk connected to the CPPI strategy, due to both price jumps and discrete time rebalancing. Moreover, we study the impact of imposing a trading constraint on the risky asset. We end the section with a study of the Constant-Mix strategy which can be considered as a specific CPPI strategy. Finally, Section 6 concludes.

2 Model Setup

We study two different dynamic strategies for asset allocation, with a strong focus on the CPPI, in a jump-diffusion framework where the price of the underlying asset may experience episodes of negative jump propagation over a short period of time. This self-contagious correlation pattern can be modeled by introducing self-exciting jumps in the underlying dynamics based on Hawkes processes. Whereas in the traditional Lévy-driven models the intensity of adverse shocks is constant, self-exciting jump processes account for the effect of time variation and clustering of jumps. The particular jump structure included in the asset dynamics allows to retain the analytical tractability of models with continuous trajectories, while also incorporating the naturally recognized downside risk of holding a strategy in the event of market crash and during the subsequent periods of sustained distress.

2.1 Jump Modeling: Hawkes Processes

Hawkes processes, first introduced by Hawkes (1971), are a class of path-dependent point processes. Like the class of Poisson processes, Hawkes processes are defined by their frequency rate, which describes the conditional expected number of jumps per unit of time. However, instead of being temporally invariant, the frequency rate of a Hawkes process is defined as a strictly positive stochastic process whose current value is determined by the number of past events weighted by a kernel function. More precisely, let $\left(\Omega, \mathcal{F}, (\mathcal{F}_t)_{0\le t\le T}, \mathbb{P}\right)$ be a filtered probability space, $\left(T_j\right)_{j\in\mathbb{N}}$ an increasing sequence of stopping times and $\left(Z_j\right)_{j\in\mathbb{N}}$ a sequence of i.i.d. random variables with common distribution f. The sequence $\left(T_j, Z_j\right)$ gives rise to a counting process defined by $H_t = \sum_{j\ge1} \mathbb{1}_{\{T_j\le t\}}$ and a marked point process given by $J_t = \sum_{j\ge1} Z_j \,\mathbb{1}_{\{T_j\le t\}}$. At each time arrival T_j, the level of the index drop is measured by a random variable Z_j. Hence, the random variable J_t tracks the sum of shocks to the asset up to time t. Adopting the notation of Jacod and Shiryaev (2003), the process J can be expressed as

$$J_t = z * \mu_t^H ,$$

where μ^H denotes the random measure of the point process H. Following Brémaud and Massoulié (1996), a non-negative $\mathcal{F}_t$−progressively measurable process $(\lambda_t)_{t\in\mathbb{R}_+}$ is called the $\mathcal{F}_t$−intensity of H if, for any $s \le t \in \mathbb{R}_+$,

$$\mathbb{E}\left[H_t - H_s|\mathcal{F}_s\right] = \mathbb{E}\left[\int_s^t \lambda_u \, du \,|\, \mathcal{F}_s\right]. \tag{1}$$

In this paper we examine two separate models for the intensity process associated with two different jump size specifications, both resulting into (H, λ) being a Markovian self-exciting Hawkes process.

First, we consider the parsimonious case where jumps arrive with $\mathcal{F}_t-$intensity defined by

$$\lambda_t = \bar{\lambda} + \int_{-\infty}^{t} g(t-s)\, dH_s\,, \tag{2}$$

where $\bar{\lambda}$ is a positive real constant, and g is a non-negative kernel function satisfying the stationary condition

$$\int_0^t g(u)\, du < 1. \tag{3}$$

As the formulation (2) is suited for every jump size specification supported on the entire real line, in the sequel we let the jump sizes be independently distributed with common Gaussian law with mean $m_J \in \mathbb{R}$ and standard deviation $\sigma_J \in \mathbb{R}_+$.

Secondly, for any jump size distribution with positive mass only on the negative line, we introduce a level effect by accommodating the intensity process responding also to the size of the jumps that have occurred in the past. In particular, we model the $\mathcal{F}_t-$intensity as a function of the magnitude of jumps so that the current level of downside jump events ramps up the intensity of future negative jumps, namely,

$$\lambda_t = \bar{\lambda} - \int_{-\infty}^{t} g(t-s)\, dJ_s\,, \tag{4}$$

where $J_t = \sum_{j=1}^{H_t} Z_j$, and g satisfies the stationary condition

$$\int_0^t g(u)\mathbb{E}\left[Z_1\right]\, du < 1. \tag{5}$$

Among this class of jumps, we consider the case where the jump sizes are independently distributed with common negative gamma law with strictly positive parameters $\kappa, \theta > \mathbb{R}_+$ and density

$$f(z) = \begin{cases} \frac{1}{\Gamma(\kappa)\theta^{\kappa}}(-z)^{\kappa-1}e^{\frac{z}{\theta}}, & \text{for } z \leq 0 \\ 0, & \text{for } z > 0. \end{cases}$$

We say that a point process is a Hawkes process if its $\mathcal{F}_t-$intensity can be formulated in the self-exciting form of (2), or in its extension given in (4).

In this paper we treat the natural case where the impact of a jump in the intensity process is governed by an exponentially decreasing function. Specifically, we consider a kernel function g of the following form

$$g(t-s) = \epsilon\, e^{-\delta(t-s)}, \quad \forall\, t \geq s\,, \tag{6}$$

where δ and ϵ are positive constants. We remark that, under the model specification (4) and (6), the intensity increases by the magnitude of the jump rescaled by the parameter ϵ every time it experiences an adverse shock and between jumps it decays exponentially with common rate δ to the level $\bar{\lambda}$. The parameter δ controls the model capability to replicate the clustered jump patterns. Indeed, by δ being assumed positive, the most recent jumps have a higher impact on the intensity path with respect to the jumps, which took place far in the past and whose contribution today is negligible. The specification (6) plays a crucial role as it results in λ being mean-reverting and Markovian jointly with the marked Hawkes process. Specifically, under an exponential decaying kernel, jump events in the two separate specifications arrive with intensity λ whose dynamics are given by

$$d\lambda_t = \delta(\bar{\lambda} - \lambda_t)dt + \epsilon\, dH_t \tag{7}$$

$$d\lambda_t = \delta(\bar{\lambda} - \lambda_t)dt - \epsilon\, dJ_t, \tag{8}$$

respectively. Note that the equivalence between the mean-reverting models specified in (7) and (8) and the defining intensity dynamics (2) and (4) under exponential decay is achieved by applying the general Itô formula for semimartingales (cf. Protter (2004), Theorem 33) to the process $f(t,\lambda) := \lambda_t e^{\delta t}$. In the case of exponential decay, the two separate stationary conditions (3) and (5) explicitly read

$$\delta > \epsilon$$

and

$$\delta > -\epsilon \int_{\mathbb{R}} z\, f(z)\, dz,$$

respectively.

Figure 2 depicts sample paths of the two intensity specifications along with the associated Hawkes process. Notice how the intensity in the top panel increases by the same amount at each jump time, while the bottom intensity scales with the jump size of J_t at each jump episode.

In the next result we look at Hawkes processes from a semimartingale viewpoint. In particular, we give a useful characterization of the pair (λ, H) in terms of semimartingale characteristics.[1]

Proposition 2.1. *A Hawkes process* $\mathbf{H} = (\lambda, H)$ *with* $\mathcal{F}_t$*−intensity admitting the form* (2) *(or* (4)*) is an* $\mathbb{R}^2$*-valued semimartingale with differential characteristics* (b, c, F) *given by*

$$b_t = \left[\delta\left(\bar{\lambda} - \lambda_t\right) + \epsilon\lambda_t \quad \lambda_t\right]^\top \quad \left(or\; b_t = \left[\delta\left(\bar{\lambda} - \lambda_t\right) - \epsilon\lambda_t \mathbb{E}\left[Z_1\right] \quad \lambda_t\right]^\top\right) \tag{9}$$

$$c_t = \begin{bmatrix} 0 & 0 \\ 0 & 0 \end{bmatrix} \tag{10}$$

$$F_t(B) = \lambda_t \mathbb{1}_B(\epsilon, 1) \quad \left(or\; F_t(B) = \lambda_t \int_{\mathbb{R}} \mathbb{1}_B(-\epsilon z, 1)\, f(z)\, dz\right), \quad B \in \mathcal{B}\left(\mathbb{R}^2\right). \tag{11}$$

Conversely, any semimartingale with differential characteristics (9)-(11) *is a Hawkes process with* $\mathcal{F}_t$*−intensity of the form* (2) *(or* (4)*).*

Remark. In the notation of Jacod and Shiryaev (2003), the compensator of the random measure $\mu^{\mathbf{H}}$ associated to the jumps of $\mathbf{H}$ reads

$$\nu^{\mathbf{H}}(]-\infty, t] \times B) = \int_{-\infty}^{t} F_s(B)\, ds. \tag{12}$$

Proof of Proposition 2.1. One easily verifies that the differential characteristics of the $\mathbb{R}^2$-valued Hawkes process $\mathbf{H} = (\lambda, H)$ equals (9)-(11). Conversely, for any semimartingale with differential characteristics (9)-(11), the process λ retains the dynamics (2). Moreover, λ is precisely the $\mathcal{F}_t$−intensity

[1] Here we adopt the notation of Kallsen (2006).

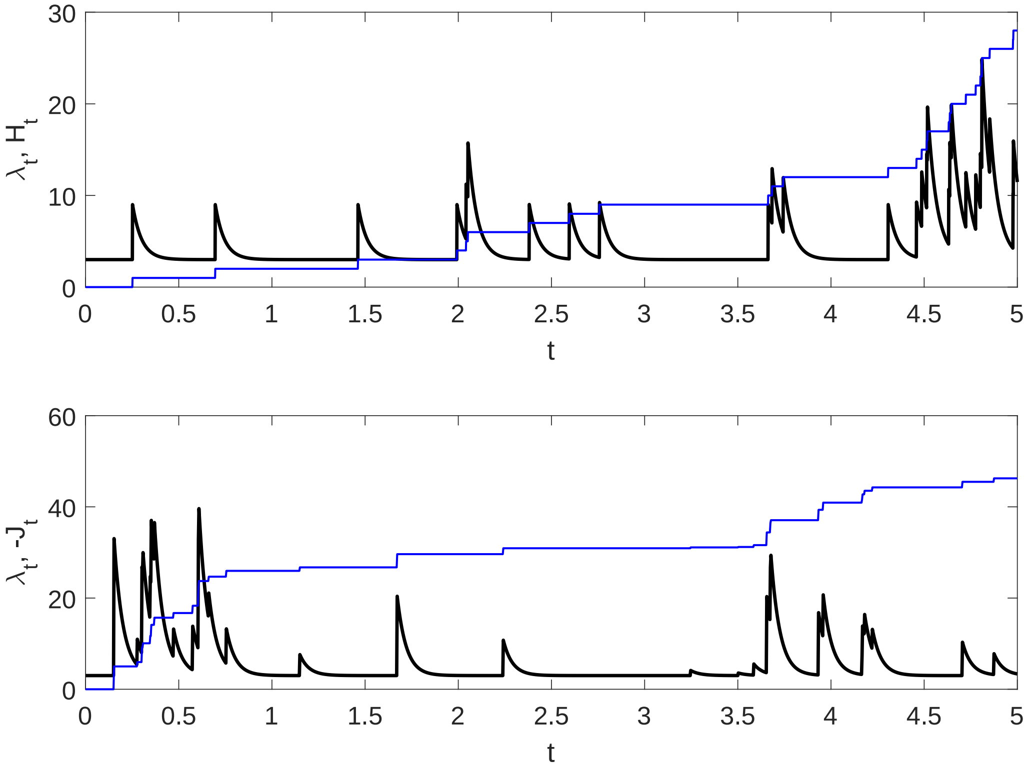

Figure 2: Sample paths of the intensities (2) (top panel) and (4) (bottom panel) and the associated Hawkes processes, H and $-J$ (blue line). In both jump specifications, the reversion level $\bar{\lambda} = \lambda_0 = 3$, the speed of mean reversion $\delta = 20$, and the jump impact $\epsilon = 6$. The jump size in (4) is drawn from a negative gamma distribution with parameters $\kappa = 2$, $\theta = 1$.

of H. In fact, the definition of the compensator of a random measure implies that $z * \mu^{\mathbf{H}} - z * \nu^{\mathbf{H}}$ is a local martingale, from which we can conclude the proof by combining the particular form of $\nu^{\mathbf{H}}$ given in (12) with Theorem T9 in Brémaud (1981). □

We state now an analogous characterization of the marked counterpart of the Hawkes process, without going through the proof that is substantially analogous to that of Proposition 2.1.

Proposition 2.2. *A marked Hawkes process* $\mathbf{J} = (\lambda, J)$ *with* $\mathcal{F}_t$*−intensity admitting the form* (2) *(or* (4)*) is an* $\mathbb{R}^2$*-valued semimartingale with differential characteristics* (b, c, F) *given by*

$$b_t = \left[\delta\left(\bar{\lambda} - \lambda_t\right) + \epsilon\lambda_t \quad \lambda_t \mathbb{E}[Z_1]\right]^\top \quad \left(or\ b_t = \left[\delta\left(\bar{\lambda} - \lambda_t\right) - \epsilon\lambda_t \mathbb{E}[Z_1] \quad \lambda_t \mathbb{E}[Z_1]\right]^\top\right) \tag{13}$$

$$c_t = \begin{bmatrix} 0 & 0 \\ 0 & 0 \end{bmatrix} \tag{14}$$

$$F_t(B) = \lambda_t \int_{\mathbb{R}} \mathbb{1}_B(\epsilon, z) f(z) dz \quad \left(or\ F_t(B) = \lambda_t \int_{\mathbb{R}} \mathbb{1}_B(-\epsilon z, z) f(z) dz\right), \quad B \in \mathcal{B}\left(\mathbb{R}^2\right). \tag{15}$$

Conversely, any semimartingale with differential characteristics (13)-(15) *is a marked Hawkes process* *with $\mathcal{F}_t$−intensity of the form (2) (or (4)).*

A remarkable property of Hawkes processes is that the characteristic function of the joint process **H** has exponential-affine form. More precisely, we have

Proposition 2.3. *The conditional characteristic function of the Hawkes process* $\mathbf{H} = (\lambda, H)$ *is given by*

$$\psi_{\mathbf{H}}(u,t,T) = \mathbb{E}\left[e^{iu\cdot \mathbf{H}_T} \mid \mathcal{F}_t\right] = e^{a(t)+\beta(t)\cdot \mathbf{H}_t}$$

for $t \le T$, and $u \in \mathbb{R}^2$. The coefficients $a(t) = a(u,t,T)$ and $b(t) = b(u,t,T)$ satisfy the following system of ODEs

$$\partial_t b_1(t) = \delta b_1(t) - \left(\theta([b_1(t) \quad b_2(t)]^\top) - 1\right) \tag{16}$$

$$\partial_t b_2(t) = 0 \tag{17}$$

$$\partial_t a(t) \;= -\delta\bar{\lambda} b_1(t), \tag{18}$$

with boundary conditions $a(T) = 0$ and $b(T) = iu$ and jump transform $\theta(\cdot)$ given by

$$\theta(\omega) = \int_{\mathbb{R}^2} e^{\omega\cdot z}\mathbf{f}(dz)\,,$$

where

$$\mathbf{f}(B) = \begin{cases} \mathbb{1}_B(\epsilon,1) & \textit{under the intensity model (7)} \\ \int \mathbb{1}_B(-\epsilon z,1)\, f(z)\, dz & \textit{under the intensity model (8)} \end{cases}, \qquad B \in \mathcal{B}\left(\mathbb{R}^2\right).$$

Remark. In the intensity formulation (8) with $Z_j \sim \mathrm{NGam}(\kappa,\theta)$, $j \ge 1$, we have the following explicit expression for the jump transform

$$\theta(b(t)) = e^{b_2(t)}\,(1-\epsilon b_1(t)\theta)^{-\kappa}, \quad \text{for } b_1(t) < \frac{1}{\epsilon\theta}.$$

2.2 Full Risky Asset Dynamics

In the previous section, we have specified the jump part of our model in a way that enables it to generate the two desirable features that are dictated by empirical observations: first, the jump activity varies through time with a direct feedback effect of jumps on the intensity of more jumps hereby assigning significant probability to the occurrence of several jumps in close succession over short periods. Second, as in the level-effect enriched intensity specification (8), the sharper the negative shock is, the bigger its impact on the intensity of future jumps will be. We now specify the full dynamics for the risky asset involved in an investment strategy by incorporating also a diffusion component which accounts for the "regular" stochastic behavior of stock prices. On $\left(\Omega, \mathcal{F}, (\mathcal{F}_t)_{0\le t\le T}, \mathbb{P}\right)$, we assume that the price process for the risky asset under the real-world probability measure $\mathbb{P}$ is modeled by a semimartingale $S = (S_t)_{t\in\mathbb{R}_+}$ satisfying

$$\frac{dS_t}{S_{t-}} = \left[r - q + \gamma_t\right] dt + \sigma\, dW_t + dJ_t^S - \mu\lambda_t\, dt\,, \tag{19}$$

where μ, σ are positive real constants, γ_t is the time-t total risk premium, $W = (W_t)_{t\in\mathbb{R}_+}$ is an adapted standard Brownian motion and $J_t^S = \sum_{j=1}^{H_t} \left(e^{Z_j} - 1\right)$. The jump size of asset log-returns, $\left(Z_j\right)_{j\in\mathbb{N}}$, is a sequence of i.i.d. random variables with density function f, which is independent of W and of all the history of jumps. Conditional on a jump arrival time T_j, the asset price at time T_j jumps by

$$S(T_j) - S(T_{j-}) = S(T_{j-})\left(e^{Z_j} - 1\right)$$

hence the relative jump size mean under the physical measure is $\mu := E\left[e^{Z_1} - 1\right] = \int_{\mathbb{R}} (e^z - 1) f(z)\, dz$. We term the model (19) H-GJDM when coupled with Gaussian jumps in asset returns, and H-NGJDM when coupled with negative gamma distributed jumps in asset returns and jump intensity.

The jump-diffusion model (19) features a twofold source of uncertainty that is driven by the Brownian motion and the self-exciting jump process. As jumps can generate clustered patterns at unpredictable times and of unforeseeable magnitude, the corresponding market model is rendered incomplete. Consequently, the risk-neutral price of a derivative is not pinpointed in a unique way as there exists an infinite class of equivalent martingale measures compatible with the no-arbitrage assumption. This in particular implies that any candidate for the change of measure from the real-world probability measure $\mathbb{P}$ to the risk-neutral probability measure $\mathbb{Q}$ would not be unique. One remedy is to specify a candidate change of measure by imposing ad hoc assumptions on the premia associated to the stock's diffusive and jump risks which maintain the model structure invariant under the change of measure. Inspired by a large body of literature on risk premia (see e.g. Pan (2002); Nicolato and Venardos (2003); Eraker (2004); Broadie et al. (2007)), we define the equivalent measure $\mathbb{Q}$ by using a candidate Radon-Nikodym derivative process of the form

$$L_t := \left.\frac{d\mathbb{Q}}{d\mathbb{P}}\right|_{\mathcal{F}_t} = \mathcal{E}\left(-\xi\sigma\, W + (\kappa - 1) * \left(\mu^X - \nu^X\right)\right)_t \tag{20}$$

for some positive constant ξ governing the premium associated to the stock diffusive risk and a strictly positive function κ controlling the premium demanded for the jump return risk. $\mathcal{E}(\cdot)$ denotes the stochastic Doléans-Dade stochastic exponential and μ^X, ν^X the random measure associated to the jumps of $X := \log(S)$ and its compensator. Further, we impose a standard jump risk premium assumption in the literature (Pan, 2002; Eraker, 2004; Broadie et al., 2007; Boswijk et al., 2015) and we assume that the jump contribution to the equity premium is entirely pinned down by the jump-size uncertainty, which amounts to the choosing of a time-independent function $\kappa = \kappa(\omega; z)$. If jump-timing risk is suppressed, the intensity of jumps is bound to remain the same under the equivalent martingale measure, leading to the same Hawkes process H driving the jump component of S.

For the two jump specifications, the process L is a $\mathbb{P}-$martingale and, in particular, $\mathbb{E}[L_t] = 1$. All the details about the change of measure are delegated to Appendices A.1 and A.2. We further assume that the class of the jump size laws is invariant under the change of measure, hence the risk-neutral jump size distribution, whose density will be denoted by $\tilde{f}$, will not be altered except through its parameters. Setting $\kappa(z) = \frac{\tilde{f}(z)}{f(z)} \mathbb{1}_{\mathrm{supp} f}(z)$, the stock price dynamics under the equivalent measure $\mathbb{Q}$ reads

$$\frac{dS_t}{S_{t-}} = \left(r - q\right) dt + \sigma\, d\tilde{W}_t + d\tilde{J}_t^S - \tilde{\mu}\,\lambda_t\, dt\,, \tag{21}$$

where $\tilde{J}_t^S = \sum_{j=1}^{H_t} \left(e^{\tilde{Z}_j} - 1\right)$ and $\tilde{\mu} := E^{\mathbb{Q}}\left[e^{\tilde{Z}_1} - 1\right] = \int_{\mathbb{R}} (e^z - 1)\, \tilde{f}(z)\, dz$. We remark that the $\mathbb{Q}-$martingality of the discounted stock price implies that

$$\gamma_t = \xi\sigma^2 + \lambda_t\left(\mu - \tilde{\mu}\right), \tag{22}$$

that is the instantaneous total equity premium can be written as the sum of two contributions: the premium associated to diffusive risk, $\xi\sigma^2$, and the premium inferred by altering the distribution of jumps, $\lambda_t\left(\mu - \tilde{\mu}\right)$. Finally, the validity of the conditions ensuring that the discounted asset price is a true martingale, and not simply a local martingale, are examined in Appendix A.3.

3 Constant Proportion Portfolio Insurance

The CPPI strategy is a dynamically adjusted trading strategy that in an ideal world puts a limit to the portfolio loss while allowing for unlimited upside. The investor will profit from the upward potential of a risky asset in a bull market while having guaranteed a fixed amount of capital G at maturity. This is achieved by investing dynamically in a "riskless" asset, typically a bond, and a risky asset, typically comprised of a stock index. Assume first that the interest rate r is constant, denote by T the maturity of the CPPI strategy and let the bond have the same maturity and nominal value G, i.e.

$$B_t = Ge^{-r(T-t)} \tag{23}$$

or, equivalently, $dB_t = rB_t dt$ with $B_0 = Ge^{-rT}$. $(B_t)_{t\in[0,T]}$ is referred to as the *bond floor* and it represents the minimal wealth that will ensure the guarantee G at maturity. Let us denote by $(V_t)_{t\in[0,T]}$ the CPPI strategy value process and assume that the guarantee is lower than the terminal value of a zero coupon bond maturing at time T, i.e. $G < V_0 e^{rT}$. Typically G is chosen to be equal to the initial investment V_0. When no leverage or liquidity constraints are in effect, as long as $V_t \geq B_t$, the stylized CPPI strategy calls for calculating the exposure to the risky asset according to the following rule

$$e_t = mC_t\,, \tag{24}$$

where m is a constant multiplier - strictly greater than 1 - reflecting the risk-appetite of the investor and C_t, termed the *cushion*, is defined as the difference between the portfolio value V_t and the bond price

$$C_t = V_t - B_t.$$

The surplus between the strategy value and the risk exposure is allocated into the non-risky asset. In case the portfolio value breaks the floor B_t at time

$$\tau = \inf\{\, t \in [0,T] \mid V_t \leq B_t\,\}, \tag{25}$$

the remaining wealth is invested in the bond and held until maturity to prevent the risk of imperiling the capital further. The risk of violating the floor is referred to as the *gap risk*.

3.1 Cushion Dynamics

Up to time τ, the value of the CPPI strategy is defined by

$$V_t = \alpha_t\, S_t + \beta_t\, B_t\,,$$

where $\alpha_t := \frac{m\,C_{t-}}{S_{t-}}$ is the number of shares held in the portfolio and $\beta_t := \frac{V_{t-}-m\,C_{t-}}{B_t}$ the remaining amount of B_t. Imposing the self-financing property of the CPPI portfolio implies in particular that

$$dV_t = \alpha_t\, dS_t + \beta_t\, dB_t. \tag{26}$$

Therefore, for any $t \leq \tau$, the cushion dynamics for this strategy can be written as (Cont and Tankov, 2009)

$$dC_t = d(V_t - B_t) = C_{t-}\left[m\,\frac{dS_t}{S_{t-}} + (1-m)\,\frac{dB_t}{B_t}\right]$$

and, in view of (19) and (23), we find

$$\frac{dC_t}{C_{t-}} = \left[\, r + m\left(-q + \gamma_t\right)\right] dt + m\,\sigma\, dW_t + m\left(dJ_t^S - \mu\,\lambda_t dt\right).$$

Denoting by $\tilde{C}_t$ the forward value of the cushion $\frac{C_t}{B_t}$ and applying the general Itô formula for semimartingales, we have

$$\frac{d\tilde{C}_t}{\tilde{C}_{t-}} = m\left(-q + \gamma_t\right) dt + m\,\sigma\, dW_t + m\left(dJ_t^S - \mu\,\lambda_t dt\right). \tag{27}$$

Defining $Y_t := Y_0 - q\,t + \int_0^t \left(\gamma_s - \mu\,\lambda_s\right) ds + \sigma\, W_t + \sum_{j=1}^{H_t}\left(e^{Z_j} - 1\right)$, equation (27) can be rewritten as

$$\frac{d\tilde{C}_t}{\tilde{C}_{t-}} = m\, dY_t$$

or, equivalently,

$$\tilde{C}_t = \tilde{C}_0\, \mathcal{E}(m\,Y)_t\,,$$

where $\mathcal{E}$ denotes the stochastic Doléans-Dade exponential. After time τ, according to the definition of the CPPI strategy, the value of the strategy is entirely invested into a zero-coupon bond to prevent further losses, i.e.

$$V_t = V_\tau e^{r(t-\tau)}, \quad \text{for any } t > \tau.$$

It follows that the cushion value, for any time t succeeding τ, can be rewritten as

$$C_t = V_\tau e^{r(t-\tau)} - G e^{-r(T-t)}$$

and, in particular,

$$\tilde{C}_t = \frac{V_\tau}{G} e^{r\,(T-\tau)} - 1\,,$$

where we can see that the forward value of the cushion process remains constant during the post-loss period.

Finally, for any date $t \in [0,T]$, we introduce a new process $C^\star$, defined as the *stopped process* of $\tilde{C}$ by the stopping time τ, i.e.

$$C^\star_t = \tilde{C}_{t\wedge\tau}\,,$$

where $t\wedge\tau := \min(t,\tau)$, and we find

$$C^\star_t = \tilde{C}_0\,\mathcal{E}(m\,Y)_{t\wedge\tau}.$$

3.2 The Probability of Loss with Continuous Trading

Modeling the gap risk is the main concern of CPPI managers since in the case of a sizable drop of the equity asset value the provider has to compensate the shortfall. Under continuous-time trading, we can exploit the analytical tractability of self-exciting jump-diffusion models to provide a semi-closed form expression for the probability that the CPPI portfolio value breaks the bond floor. A loss in the CPPI strategy occurs when there exists a time t prior to maturity such that $V_t \le B_t$. The probability of this event to happen is called *gap risk*. Given the equivalence between the event $V_t \le B_t$ and $C^\star_t \le 0$, we have that $C^\star_t \le 0$ for some $t\in[0,T]$ if and only if $\Delta Y_t \le -\frac{1}{m}$ for some $t\in[0,T]$ (Cont and Tankov, 2009).

Using the previous argument, we have that

$$P\left(\{\exists t\in[0,T]: V_t \le B_t\}\right) = 1 - P\left(\#\left\{t\in[0,T]: \Delta Y_t \le -\frac{1}{m}\right\} = 0\right).$$

Hence, the quantification of the gap risk is reduced to the computation of the probability that, throughout the life of the strategy, there occurs no jumps with size lower or equal to $-\frac{1}{m}$.

We recall that Y is of the form

$$Y_t := Y^c_t + Y^J_t\,,$$

where $Y^c_t := Y_0 - q\,t + \int_0^t \left(\gamma_s - \mu\,\lambda_s\right)ds + \sigma\,W_t$ is its continuous component and $Y^J_t := \sum_{j=1}^{\tilde{N}_{\Gamma_t}}\left(e^{Z_j}-1\right)$ is the independent jump part which serves to capture large and clustered events. The jump sizes $\left(Z_j\right)_{j=1,\cdots,\tilde{N}_{\Gamma_t}}$ are in particular i.i.d. random variables with cumulative distribution function F.

Proposition 3.1 (Probability of loss)**.** *The probability of breaching the floor is given by*

$$P\left(\{\exists\, t\in[0,T]: V_t \le B_t\}\right) = 1 - \sum_{n=0}^{\infty} q_m^n P\left(H_T = n\right)\,, \tag{28}$$

where $q_m := 1 - F\left(\log\left(1-\frac{1}{m}\right)\right)$.

Proof. The probability of k jumps incurring in the time period $[0,T]$ is given

$$\begin{aligned} P\left(\#\left\{t\in[0,T]:\Delta Y_t\le -\frac{1}{m}\right\}=k\right) &= P\left(\#\left\{e^{Z_1}-1,\cdots,e^{Z_{H_T}}-1\le -\frac{1}{m}\right\}=k\right) \\ &= P\left(\#\left\{Z_1,\cdots,Z_{H_T}\le \log\left(1-\frac{1}{m}\right)\right\}=k\right) \\ &= \sum_{n=0}^{\infty} P\left(\#\left\{Z_1,\cdots,Z_n\le \log\left(1-\frac{1}{m}\right)\right\}=k\right) P\left(H_T=n\right) \\ &= \sum_{n=0}^{\infty}\binom{n}{k} p_m^k q_m^{n-k}\, P\left(H_T=n\right)\,, \end{aligned}$$

where $p_m := 1-q_m$. When $k=0$, the formula reduces to

$$P\left(\#\left\{t\in[0,T]:\Delta Y_t\le -\frac{1}{m}\right\}=0\right)=\sum_{n=0}^{\infty} q_m^n\, P\left(H_T=n\right).$$

□

The probability mass function, $P(H_T=\cdot)$, appearing in (28) can be computed from the probability generating function of H_T, defined as

$$G(v)=\mathbb{E}\left[v^{H_T}\right]=\sum_{n=0}^{+\infty} P\left(H_T=n\right)v^n\,, \tag{29}$$

for $v\in\mathbb{R}$ and $n\in\mathbb{N}\cup\{0\}$. Note that (29) is a power series with radius of convergence $R\ge 1$, meaning that G is well-defined for every $v\in[-1,1]$. The function G is linked to the characteristic function of the joint process $\mathbf{H}$ by the following relation

$$G(v)=\psi_{\mathbf{H}}\left(\begin{bmatrix}0 & -i\log(v)\end{bmatrix}^\top,0,T\right),\qquad v\in(0,1) \tag{30}$$

and

$$G(0)=\lim_{v\to 0+}\psi_{\mathbf{H}}\left(\begin{bmatrix}0 & -i\log(v)\end{bmatrix}^\top,0,T\right). \tag{31}$$

Equations (30)-(31) can be combined with Equation (29) to retrieve the mass probability function needed in (28). For a fixed order N, consider the polynomial $p(x)=a_1x+\ldots+a_Nx^N$ resulting from truncating (29), where $a_n=P(H_T=n)$, $n=1,\ldots,N$, are unknown. Then, fit p to an N-dimensional grid of values of G, evaluated at arbitrary – e.g. equispaced – points in the interval $[0,1]$ through (30). Provided that N is suitably large, the obtained estimates of $a_1,\ldots,a_N$ will then approximate $P(H_T=1),\ldots,P(H_T=N)$, respectively.

Applying this procedure with $N=10$, we determine the loss probability corresponding to different levels of the multiplier, which is reported in Figure 3. We observe that the heavier tail of the negative gamma distribution has a dramatic impact on the probability of a loss for multipliers ranging from around 3 to 7. In particular for multipliers below 5 the probability of realizing jumps to the price smaller than $-1/m$ is essentially zero for the given parameters in the H-GJDM. It is important for the investor to quantify the gap risk as a function of the multiplier in order to choose a multiplier

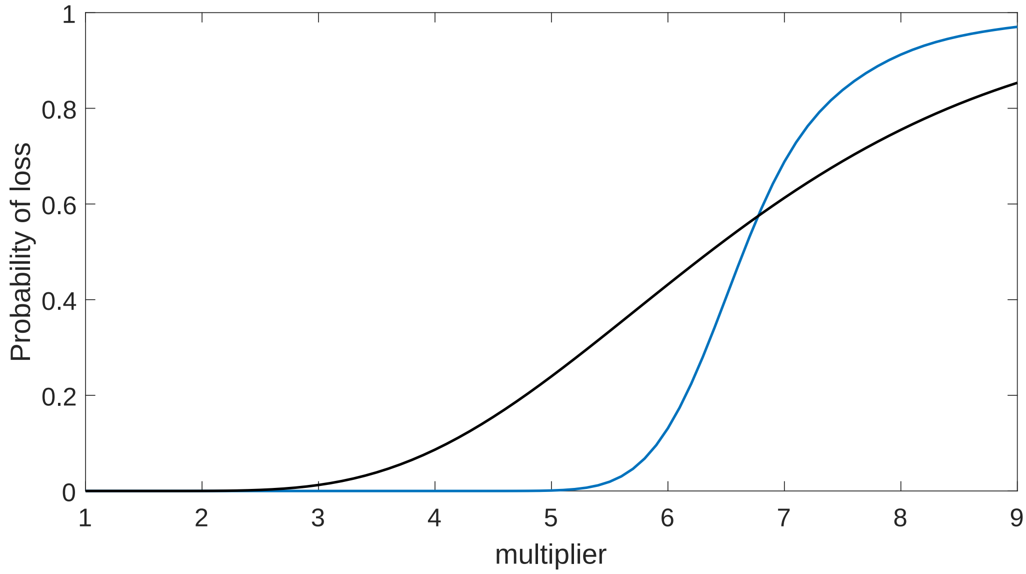

Figure 3: Probability of loss as function of the multiplier m in the H-GJDM (blue line) and in the H-NGJDM (black line) on January 5, 2015. The model parameters are reported in Table 1, while the CPPI contract has $T = 5$ years, $m = 5$, $V_0 = 1$, $G = 1$, $r = 0.01$, and $q = 0$.

corresponding to her risk appetite.

4 Calibration of the Models

In order to obtain reasonable parameter sets for the model specifications we calibrate the models to options data on the SPX index. Besides the two Hawkes driven specifications, H-GJDM and H-NGJDM, we consider two models where the jumps are driven by compound Poisson processes. For the two fixed intensity models we let the jumps be Gaussian and negative gamma distributed and label the two specifications as CP-GJDM and CP-NGJDM, respectively. The two compound Poisson models are included in order to be able to compare the results of the contagion specifications with more traditional jump models. The option quotes are collected from OptionMetrics and as the option price we use the mid of bid and ask prices. The discount curve and the constant dividend yield q are derived from option quotes around at-the-money (ATM) via the Put-Call parity. The option data is filtered in a number of ways: first, we only consider out-of-the-money (OTM) options. Second, we remove option quotes where the bid price is zero, options where the absolute moneyness is greater than 40%, i.e. $| \frac{K}{S} - 1 | > 0.40$, and options with nominal bid-ask spread greater than \$10. On this data set we filter away call options violating the no-arbitrage conditions (Carr and Madan, 2005)[2]

$$C_t(S_t;T,K_j) > \max\left\{0, S_t e^{-\int_t^T q_s ds} - K_j e^{-\int_t^T r_s ds}\right\} \tag{32}$$

$$\frac{C_t(S_t;T,K_{j-1}) - C_t(S_t;T,K_j)}{K_j - K_{j-1}} \in \left[0, e^{-\int_t^T r_s ds}\right] \tag{33}$$

$$\frac{C_t(S_t;T,K_{j-1}) - C_t(S_t;T,K_j)}{K_j - K_{j-1}} - \frac{C_t(S_t;T,K_j) - C_t(S_t;T,K_{j+1})}{K_{j+1} - K_j} \geq 0\,, \tag{34}$$

where $K_{j-1} < K_j < K_{j+1}$.

Model option prices can be computed with Fourier methods once the characteristic function of the log-returns is available. Let $S_t = S_0\, e^{\int_0^t (r_s - q) ds + \tilde{X}_t}$ where

$$\tilde{X}_t = -\frac{1}{2}\sigma^2\, t + \sigma\, \tilde{W}_t + \tilde{J}_t - \tilde{\mu}\int_0^t \lambda_s\, ds, \quad \tilde{X}_0 = 0.$$

Here we relate the characteristic function of $\tilde{X}$ to call option prices via the Lewis formula (Lewis, 2001)

$$C_t(S_t, K, T) = S_t e^{-q(T-t)} - \frac{\sqrt{S_t K} e^{-\frac{\int_t^T (r_s+q) ds}{2}}}{\pi} \int_0^\infty \frac{\mathcal{R}\left(e^{\mathrm{i}uk}\psi\left(u - \frac{\mathrm{i}}{2}, t, T\right)\right)}{u^2 + \frac{1}{4}}\, du\,, \tag{35}$$

where $k = \log\left(\frac{S_t}{K}\right) + \int_t^T \left(r_s - q\right)\, ds$ and

$$\psi(u,t,T) = \mathbb{E}^{\mathbb{Q}}\left[e^{\mathrm{i}u\,\tilde{X}_T} \mid \mathcal{F}_t\right]$$

is the characteristic function of the log-returns conditional on the information at time t. The contagion specifications considered can be embedded into the affine jump-diffusion framework of Duffie et al. (2000). Thus, under technical conditions, the characteristic function is available up to the numerical solution of a system of ODEs. Since the risky asset dynamics is comprised of the independent diffusive and of the Hawkes dynamics, the conditional characteristic function takes the form of a product

$$\psi(u,t,T) = \psi_1(u,t,T)\psi_2(u,t,T) \tag{36}$$

$$= e^{-\frac{1}{2}\sigma^2(T-t)u(\mathrm{i}+u) + ui\left(\sigma\tilde{W}_t - \frac{1}{2}\sigma^2 t\right)} e^{a(v,t,T) + b(v,t,T)\cdot Y_t}\,, \tag{37}$$

where $v = [0 \quad \mathrm{i}u]^\top$ and $Y_t = \left[\lambda_t \quad -\tilde{\mu}\int_0^t \lambda_s\, ds + \tilde{J}_t\right]^\top$.[3] The coefficients functions $a(t) = a(v,t,T)$ and

[2]For the put option quotes we convert the prices into call options via the Put-Call parity and apply the arbitrage conditions stated in equations (32)-(34).

[3]Adopting the notation of Duffie et al. (2000), the process Y_t is a 2-dimensional affine process with non-null coefficients

$$(K_0, K_1) = \left([\delta\,\bar{\lambda} \quad 0]^\top, \begin{bmatrix} -\delta & 0 \\ -\tilde{\mu} & 0 \end{bmatrix}\right)$$

$$(l_0, l_1) = \left(0, [1 \quad 0]^\top\right).$$

$b(t) = b(v,t,T)$ solve

$$\partial_t b_1(t) = \delta b_1(t) + \tilde{\mu} b_2(t) - \left(\theta([b_1(t) \quad b_2(t)]^\top) - 1\right) \tag{38}$$

$$\partial_t b_2(t) = 0 \tag{39}$$

$$\partial_t a(t) \ = -\delta \bar{\lambda} b_1(t), \tag{40}$$

with boundary conditions $a(T) = 0, b_1(T) = 0$ and $b_2(T) = \mathrm{i}u$. For $\omega \in \mathbb{C}^2$, the jump transform $\theta(\cdot)$ equals

$$\theta(\omega) = \int_{\mathbb{R}^2} e^{\omega \cdot z} \mathbf{f}(dz)\,,$$

where

$$\mathbf{f}(B) = \begin{cases} \int \mathbb{1}_B(\epsilon, z) \tilde{f}(z)\, dz & \text{if} \quad \tilde{Z}_j \sim \mathcal{N}(\tilde{m}_J, \sigma_J) \\ \int \mathbb{1}_B(-\epsilon\, z, z) \tilde{f}(z)\, dz & \text{if} \quad \tilde{Z}_j \sim \mathrm{NGam}(\kappa, \rho\theta) \end{cases}, \qquad B \in \mathcal{B}\left(\mathbb{R}^2\right).$$

We calibrate by minimizing the sum of squared errors between model and market mid prices

$$\mathrm{SSE} = \sum \left(Q^{\mathrm{Model}} - Q^{\mathrm{Market}}\right)^2\,,$$

where Q refers to an OTM put or call option price. We compare the calibration performance via the Average Relative Pricing Error (ARPE) on implied volatilities, defined as

$$\mathrm{ARPE} = \frac{1}{\{\#\text{ options}\}} \sum_{\text{options}} \frac{|\mathrm{IV}^{\mathrm{Model}} - \mathrm{IV}^{\mathrm{Market}}|}{\mathrm{IV}^{\mathrm{Market}}}.$$

Figure 4 depicts the fit to the observed implied volatility smiles on January 5, 2015. We see that the added flexibility of the Hawkes specifications improves the fit significantly compared to the constant intensity cases. The Hawkes specifications are performing well although the volatility σ is constant as the self-exciting behavior of the intensity introduces both randomness in the quadratic variation process of the log-returns and generates the leverage effect, i.e. two features typically added via a stochastic volatility factor. For the two models with constant intensity the smile flattens too fast, as both models imply independent and identically distributed increments in the log-returns.

5 Simulation Study

In this section we analyze via simulation the performance of the CPPI strategy under different assumptions imposed on the rebalancing frequency. We compare the results when employing the Hawkes driven jump-diffusion model (19) and its constant intensity counterpart. First, we consider the simplest case where the CPPI is rebalanced on a fixed time grid.

5.1 Pricing of the Gap Risk for Discretely Rebalanced CPPI Strategies

Consider the fixed tenor grid $\mathcal{T} = \{T_0, T_1, \ldots, T_n\}$ at which the CPPI is rebalanced, where $T_n = T$ is the maturity of the CPPI. In this case the time point of the floor violation can be defined as $\bar{\tau} =$

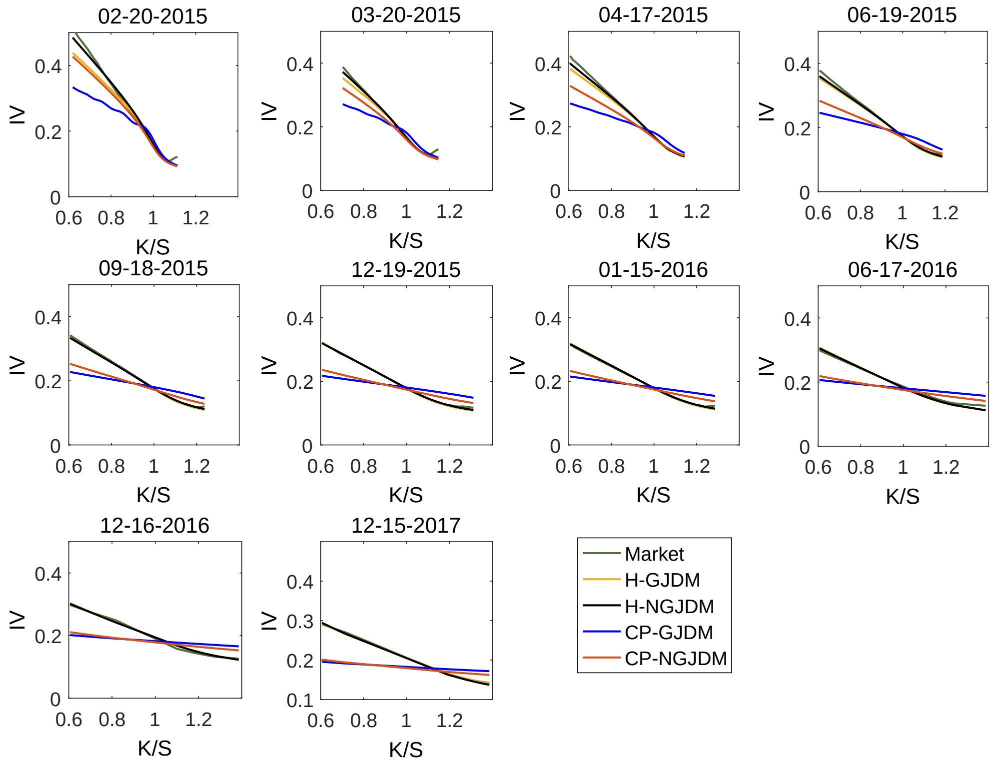

Figure 4: Fit of the four model specifications to the observed option implied volatility smiles on January 5, 2015.

$\inf\{t \in \mathcal{T} \mid V_t \leq B_t\}$. Typically the issuer of the CPPI guarantees that the investor receives as minimum the terminal capital G. In this case the issuer will charge an initial fee equal to the present value of the CPPI loss

$$P^{\text{Fee}} = -\mathbb{E}^{\mathbb{Q}}\left[\min\{C_T, 0\}\, e^{-rT}\right].$$

In the stylized CPPI the amount invested in the risky asset can exceed the value of the strategy $mC_t > V_t$ which then has to be funded with a short position in the risk-free bond. In practice the issuer will put a constraint on the leverage restricting the exposure to the risky asset according to the rule

$$e_t = \min\{mC_t, bV_t\}, \quad b \in (0, m]. \tag{41}$$

In the analysis we allow for leverage up to 100% and put $b = 2$.

In order to illustrate the impact of contagion we calibrate the Hawkes-driven specifications to option surfaces on 12 different dates divided into three categories: pre-crisis, crisis, and post-crisis periods. For the calibrated models we compute the gap risk fee under different assumptions imposed on the rebalancing frequency. For comparison we consider more traditional constant intensity jump models where the jump distribution parameters and the volatility σ are set equal to those calibrated for the corresponding Hawkes model, while the remaining intensity parameter is left free to calibrate

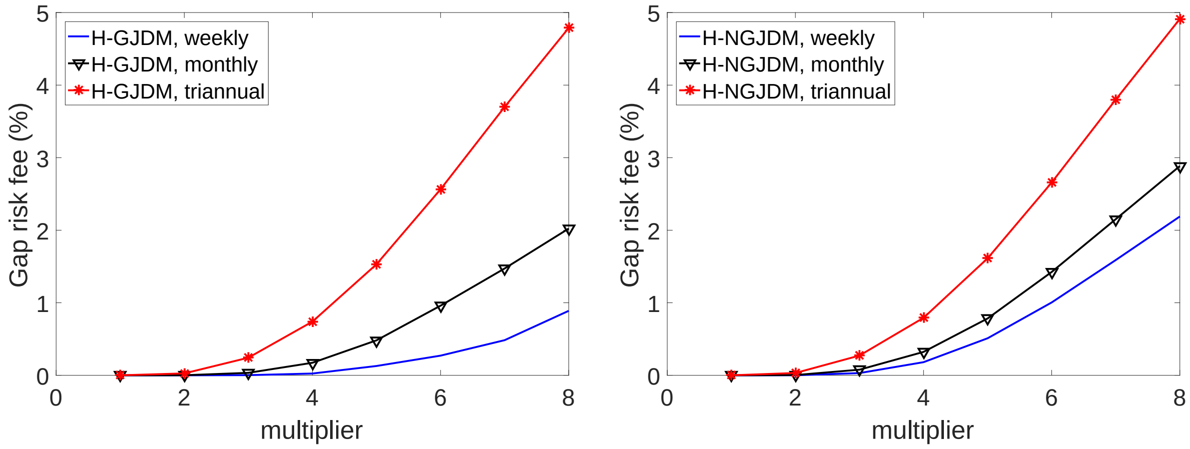

Figure 5: Gap risk fee as function of the multiplier in the H-GJDM (left panel) and in the H-NGJDM (right panel). Both model specifications are calibrated to options data from January 5, 2015.

to the given option surface. The parameter fixing is imposed in order to have models that only differ in their jump intensity structure.

We consider a CPPI strategy with maturity $T = 5$ years, multiplier $m = 5$, initial investment $V_0 = 1$ and a protection level of 100%, i.e. $G = 1$. We further suppose $r = 0.01$ and a zero dividend yield q. Inspection of Table 1 reveals a number of observations: first, the gap risk fee increases as the rebalancing frequency declines, reflecting the increased probability of the portfolio value V breaching the barrier between trading dates. Second, except for a few crisis dates and for very frequent rebalancing, the Hawkes specification with Gaussian jumps assigns a higher gap risk fee compared to the fixed intensity counterpart irrespective of the rebalancing frequency. Also, Table 1 clearly illustrates that failing to take the contagious nature of jumps into account during quiet periods on financial markets will lead to a significantly underestimated fee. Compared to the fixed jump intensity models and in periods of low jump activity, the Hawkes specifications assign more probability to the events that many jumps occur within two trading dates, as the first jump occurrence will push up the intensity of subsequent jumps. In contrast, in more distressed markets both the fixed intensity and the self-exciting intensity models start out with a high level of jump activity giving rise to a gap risk fee of the same magnitude. For the negative gamma jump models we observe the same overall picture although not as clear as for the Gaussian jumps. Now the fixed intensity model gives rise to the highest fee on more occasions although not by much. As also indicated by Figure 3, for frequent rebalancing the fee under the H-NGJDM is significantly higher in magnitude compared to the H-GJDM, since the former assigns higher probability to the event that the floor is violated in only one jump.

For the two contagion specifications, Figure 5 depicts the gap risk fee as a function of the risk-multiplier m on January 5, 2015. It clearly shows both the positive relation between the fee and the multiplier, and the fee and the space between rebalancing dates.

Table 1: Gap risk fees, equidistant rebalancing.

GAUSSIAN JUMPS																
		Calibrated parameters									Gap risk fee (%)					
		σ	λ	λ_0	$\bar{\lambda}$	δ	ϵ	m_J	σ_J	ARPE (%)	d	w	2w	m	3m	4m
Pre-crisis (2007)	Jan 05	0.08		0.64	0.79	9.23	6.24	-0.1	0	4.34	0	0.04	0.12	0.31	0.85	1.03
		0.08	1.44					-0.1	0	16.1	0	0	0.01	0.03	0.16	0.23
	Apr 05	0.07		1.23	0.97	11.05	7.67	-0.09	0	4.1	0	0.03	0.09	0.27	0.79	0.98
		0.07	2					-0.09	0	16.44	0	0	0.01	0.02	0.12	0.18
	Jul 06	0.07		3.36	1.55	4.92	3.81	-0.07	0.01	2.94	0	0.01	0.03	0.12	0.56	0.76
		0.07	2.71					-0.07	0.01	14.14	0	0	0	0.01	0.07	0.11
	Oct 05	0.08		2.34	1.08	4.14	3.16	-0.1	0.04	3.35	0.01	0.1	0.2	0.43	1.16	1.45
		0.08	2.64					-0.1	0.04	12.04	0.02	0.06	0.11	0.23	0.63	0.8
Crisis (2008-2009)	Sep 05	0.11		8.05	1.34	3.85	3.64	-0.07	0.01	3.44	0	0.02	0.07	0.25	1.07	1.45
		0.11	7.74					-0.07	0.01	9.48	0	0.01	0.04	0.15	0.8	1.12
	Dec 05	0.18		20	1.56	8.19	6.89	-0.13	0.01	2.42	0.06	0.55	1.15	2.38	5.75	6.96
		0.18	10.7					-0.13	0.01	15.27	0.1	0.53	1.02	2.19	5.57	6.87
	Apr 03	0.18		13.86	1.22	5.33	4.96	-0.09	0.03	2.6	0.03	0.21	0.48	1.1	3.13	3.95
		0.18	10.64					-0.09	0.03	9	0.06	0.25	0.53	1.21	3.42	4.33
	Jun 04	0.13		7.79	1.29	5.06	4.67	-0.1	0.02	3.39	0.01	0.13	0.32	0.78	2.37	3.02
		0.13	6.92					-0.1	0.02	11.69	0.02	0.1	0.24	0.62	1.95	2.51
Post-crisis (2015)	Jan 05	0.07		2.06	0.61	3.15	2.93	-0.12	0.03	2.33	0.01	0.13	0.24	0.48	1.23	1.53
		0.07	1.86					-0.12	0.03	13.27	0.01	0.08	0.15	0.29	0.70	0.88
	Apr 02	0.06		2.72	0.93	4.2	4.01	-0.09	0.01	5.07	0	0.04	0.11	0.31	1.03	1.35
		0.06	2.92					-0.09	0.01	19.4	0	0.01	0.02	0.08	0.34	0.48
	Jul 02	0.06		3.15	1.14	5.3	4.62	-0.08	0.02	2.86	0	0.04	0.11	0.31	1.04	1.33
		0.06	3.38					-0.08	0.02	18.6	0	0.01	0.03	0.08	0.34	0.47
	Aug 07	0.06		2.89	1.43	6.48	5.58	-0.08	0	3.69	0	0.02	0.08	0.27	1.02	1.33
		0.06	3.82					-0.08	0	19.3	0	0	0.01	0.03	0.22	0.32
NEGATIVE GAMMA DISTRIBUTED JUMPS																
		Calibrated parameters									Gap risk fee (%)					
		σ	λ	λ_0	$\bar{\lambda}$	δ	ϵ	κ	θ	ARPE (%)	d	w	2w	m	3m	4m
Pre-crisis (2007)	Jan 05	0.07		5.29	3.33	2.36	68.65	0.44	0.06	3.25	0.21	0.24	0.28	0.38	0.69	0.82
		0.07	7.21					0.44	0.06	11.90	0.23	0.25	0.27	0.31	0.45	0.52
	Apr 05	0.06		5.40	2.39	2.39	59.19	0.80	0.04	3.16	0.08	0.10	0.14	0.21	0.49	0.62
		0.06	6.61					0.80	0.04	11.87	0.09	0.10	0.12	0.16	0.30	0.37
	Jul 06	0.08		6.71	3.15	0.67	32.28	0.16	0.13	5.21	0.85	0.87	0.90	0.97	1.17	1.26
		0.08	7.34					0.16	0.13	6.36	1.00	1.02	1.03	1.07	1.20	1.26
	Oct 05	0.08		4.83	2.06	2.24	34.92	0.82	0.06	3.69	0.41	0.48	0.55	0.72	1.26	1.46
		0.08	5.19					0.82	0.06	9.02	0.52	0.56	0.61	0.72	1.07	1.22
Crisis (2008-2009)	Sep 05	0.10		15.43	2.30	4.29	85.89	3.00	0.02	3.65	0	0.03	0.09	0.28	1.11	1.49
		0.10	14.69					3.00	0.02	9.10	0	0.03	0.07	0.20	0.86	1.17
	Dec 05	0.19		19.87	1.63	7.34	51.84	4.92	0.02	3.39	0.31	0.92	1.53	2.73	5.90	7.04
		0.19	10.54					4.92	0.02	15.37	0.42	0.97	1.56	2.72	6.11	7.40
	Apr 03	0.16		19.92	1.72	7.88	47.31	7.44	0.02	3.26	0.25	0.97	1.65	2.95	6.32	7.41
		0.16	6.06					7.44	0.02	9.23	0.27	0.65	1.05	1.86	4.17	5.00
	Jun 04	0.13		14.76	2.25	4.32	76.15	1.13	0.05	3.21	0.26	0.43	0.62	1.06	2.45	3.03
		0.13	13.03					1.13	0.05	9.59	0.38	0.53	0.70	1.11	2.40	2.92
Post-crisis (2015)	Jan 05	0.07		7.62	1.81	2.80	64.96	0.57	0.07	1.69	0.43	0.51	0.60	0.78	1.37	1.61
		0.07	6.28					0.57	0.07	11.27	0.59	0.64	0.67	0.77	1.07	1.19
	Apr 02	0.06		7.17	2.13	2.83	79.18	0.50	0.07	5.47	0.38	0.45	0.53	0.71	1.29	1.52
		0.06	7.37					0.50	0.07	14.27	0.50	0.54	0.58	0.66	0.93	1.05
	Jul 02	0.06		5.60	1.95	4.90	81.48	1.68	0.03	2.84	0.05	0.13	0.22	0.42	1.10	1.38
		0.06	5.89					1.68	0.03	16.30	0.07	0.09	0.13	0.21	0.49	0.62
	Aug 07	0.06		5.55	2.23	4.53	85.05	1.82	0.03	3.85	0.02	0.08	0.15	0.33	0.96	1.23
		0.06	6.74					1.82	0.03	16.65	0.03	0.05	0.07	0.13	0.36	0.47

The table reports calibrated parameters for the H-JDM (upper row), and the CP-JDM (lower row) and the corresponding CPPI upfront gap risk fees for six different equidistant rebalancing rules: daily (d), weekly (w), fortnightly (2w), monthly (m), quarterly (3m), triannual (4m). We examine three market scenarios: the pre-crisis period (relative to the year 2007), the crisis (spanning from late 2008 to 2009), and the post-crisis period (referring to the year 2015). ARPEs on implied volatilities and gap risk fees are reported in percentage. *Remark:* Number of simulations: 10^6.

5.2 CPPI Subject to Discrete Trading

Good gap risk measurement is essential for the bearer of the gap risk, both for risk management purposes and to determine the amount of risk capital required for holding the risk of the CPPI strategy. We measure via simulation the gap risk caused by both a discrete rebalancing rule and the presence of contagious downward jumps in the price of the risky asset embedded in the CPPI portfolio. Risk probabilities and expectations are fair-valued under the real-world measure $\mathbb{P}$. To achieve this, we use the parameters determined from the calibration to S&P 500 quoted option prices and estimated diffusive and jump risk premia to recover the objective dynamics (19) as outlined in Section 2. We simulate the risky asset dynamics using a plausible mean price jump risk premium per unit jump intensity of $\mu - \tilde{\mu} = 44$ basis points per year and a diffusive risk premium per unit volatility risk of $\zeta\sigma = 0.55$ per year, which are consistent with the estimation results provided by Pan (2002) and Balder et al. (2009). We note here that the total jump risk premium in the asset dynamics is stochastic in the contagion specifications via the multiplication by the intensity of jumps in the asset dynamics. In stressed scenarios associated with high λ_t the jump risk premium is high as also documented empirically (Todorov, 2010).

For the Gaussian jump specifications and for the different rebalancing frequencies, Table 2 reports the risk measures, the VaR at the 99% level, the expected shortfall at the 99% level, the expected loss conditioned on a loss, and finally the probability of a loss. Focusing on the columns showing the probability of a loss we observe that except for a few crisis dates, the Hawkes process driven model gives rise to a higher loss probability compared to the fixed intensity model. With the set of calibrated parameters for the Gaussian jumps and with frequent rebalancing one needs more than one jump to occur between two trading dates in order to breach the barrier.[4] In the non-crisis periods with low fixed intensity, λ, the probability of jump clustering is essentially zero in contrast to the self-exciting jump specification, where the jump intensity can build up over time as jumps are realized.

An interesting discrepancy between the fixed intensity and the self-exciting intensity models is revealed by inspection of the conditional expected loss columns in Tables 2 and 3. In general for both jump distributions we see that for frequent rebalancing the fixed intensity specifications lead to the highest conditional expected loss while the ranking of the models is swapped for more infrequent rebalancing. However, for almost all dates and all rebalancing frequencies, the Hawkes specifications have significantly higher 99% VaR, 99% ES. This can be explained by the self-exciting nature of the jump intensity. A violation of the floor will typically occur in connection with a negative jump to the price of the risky asset, which will ramp up the intensity making it more likely for the strategy to incur more negative shocks. This contrasts the fixed intensity model where a violation of the guarantee does not imply an increased probability of further jumps to happen. Figure 6 depicts the simulated distributions of the cushion value at the maturity of the CPPI for the two specifications with Gaussian jumps and with weekly rebalancing. Only the negative cushion values are shown. Focusing on the unconditional distributions it is clear that compared to the CP-GJDM, the H-GJDM has the highest loss probability and the greatest tail risk measures as it has both more mass on the negative line and a heavier tail to the left. In contrast, when conditioning on a loss occurring the H-GJDM has most of

[4] With frequent rebalancing the risk of breaching the floor due to large negative continuous movements is small.

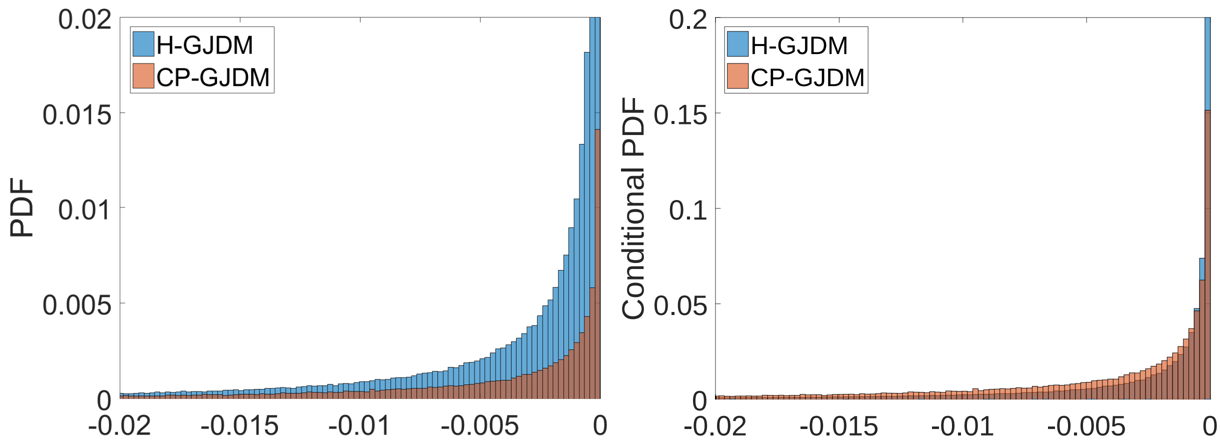

Figure 6: Simulated distribution of the CPPI's cushion at maturity (left panel) and simulated distribution of the CPPI's cushion at maturity conditioned on a loss occurring (right panel), for the H-GJDM and for the CP-GJDM. Both distributions are zoomed in on the negative real line and the result of weekly rebalanced positions in the risky and risk-free asset.

its mass around zero while the CP-GJDM distribution is more spread out on the negative line. When the CPPI portfolio is rebalanced frequently and since more than one jump needs to occur in order for the CPPI to breach the barrier, typically in the H-GJDM the stock index will experience negative jumps preceding the violation of the floor in order for the intensity to build up (top panel in Figure 7). Hence, the CPPI manager will have sold off the risky exposure leading up to the breach resulting in a small loss. This contrasts the fixed intensity specification where the barrier is rarely breached, but when it happens the risky exposure is typically at a high level leading to a big loss.

The results for the negative gamma distributed jumps reported in Table 3 share the same qualitative behavior as the Gaussian jump models. Again, we see that the heavier tails of the negative gamma distribution lead to higher risk measures when rebalancing is frequent.

5.3 CPPI Based on Risky Assets with Low Liquidity

The assumption that the CPPI manager can sell and buy unlimited amounts of the risky asset from day to day might be too strict in practice. Often portfolio managers are forced to split a given trade into smaller pieces to avoid an undesired price impact. In this Section we consider a simple version of an execution of a block trade in a market with low liquidity. In specific, we assume that the daily trade in the risky asset is limited, here represented as a fraction Θ of the notional G of the CPPI, while the risk-free asset can be traded daily in any desired quantity.[5] Let e_t denote the exposure to the risky asset computed according to the trading rule in equation (41) and by $\bar{e}_t$ the actual exposure

[5] For a study focused on optimal execution in a framework utilizing Hawkes processes to model the order book flow, the reader is referred to Alfonsi and Blanc (2016).

at time t. Then the exposure at time $t+1$ is computed as follows

$$\bar{e}_{t+1} = \begin{cases} \bar{e}_t + \Theta G & \text{if} \quad e_{t+1} - \bar{e}_t > \Theta G \\ e_{t+1} & \text{if} \quad e_{t+1} - \bar{e}_t \in [-\Theta G, \Theta G] \\ \bar{e}_t - \Theta G & \text{if} \quad e_{t+1} - \bar{e}_t < -\Theta G \end{cases} .$$

Hence, the CPPI manager can be forced to sell/buy the risky assets in smaller portions over several days after a big move in the risky asset in order to arrive at the target exposure given by (41).

Table 4 reports the gap risk fee computed under the liquidity constrained trading in the risky asset with $\Theta = 0.05$. Compared to the fees under daily rebalancing but with no liquidity constraint, all the fees have increased. Also the ranking of the models has swapped on many dates as the contagion specifications give rise to the highest fee. Still, the impact of contagion is not considerable. In contrary a clearer picture is revealed from inspection of the Table 5. In general the two self-exciting jump specifications lead to significantly higher risk measures; VaR and expected shortfall, even though the rebalancing is performed on a daily basis. Especially, the expected shortfall is greater up to a factor 10 on many dates. Hence, if the CPPI is based on a risky asset with low liquidity, neglecting to take the contagious nature of jumps into account will significantly underestimate the risks associated with the CPPI.

Figure 7 depicts the values of the CPPI strategy's factors in the dual case of the stylized CPPI and of its illiquidity-integrated companion. The middle panel illustrates a delay affecting the risky exposure due to trades of risky asset being constrained. A consequent deterioration of the CPPI value is illustrated in the bottom panel, where the floor violation is rendered more severe when the liquidity constraint is in effect.

5.4 Constant-Mix Strategy

As long as the CPPI is above the floor, it is a convex/momentum strategy that mandates the selling of stocks as they fall and the buying of stocks as they rise. Accordingly, it combines capital protection with favorable performance in bull markets. The CPPI has been criticized for the fact that once the CPPI value crosses the floor, the wealth is locked in the risk-free asset until the maturity.

A concave companion of the CPPI, called Constant-Mix strategy, is an example of dynamic asset allocation which, first: does not allow for leverage and second: will always maintain a position in the risky asset. The Constant-Mix strategy dynamically allocates a fixed and pre-determined percentage of the wealth at investors' disposal in stocks and the remaining is invested in bonds. In particular the investment rule which intertwines positions in bonds with positions in stocks underlying a Constant-Mix strategy can be viewed as a special case of the CPPI where the exposure to the risky asset is computed according to the rule in equation (24), with the bond floor being zero valued and the multiplier m taking value between 0 and 1. The concavity of the strategy stems from the fact that the allocation rule is designed to sell the excess between the market and the target exposure and invest the proceeds in bonds if the stock rises in value. On the contrary, if the stock price topples, the wealth gap between the market and the target exposure is financed by selling a corresponding quantity of bonds. Therefore the Constant-Mix strategy inherently does not take any return advantage of either

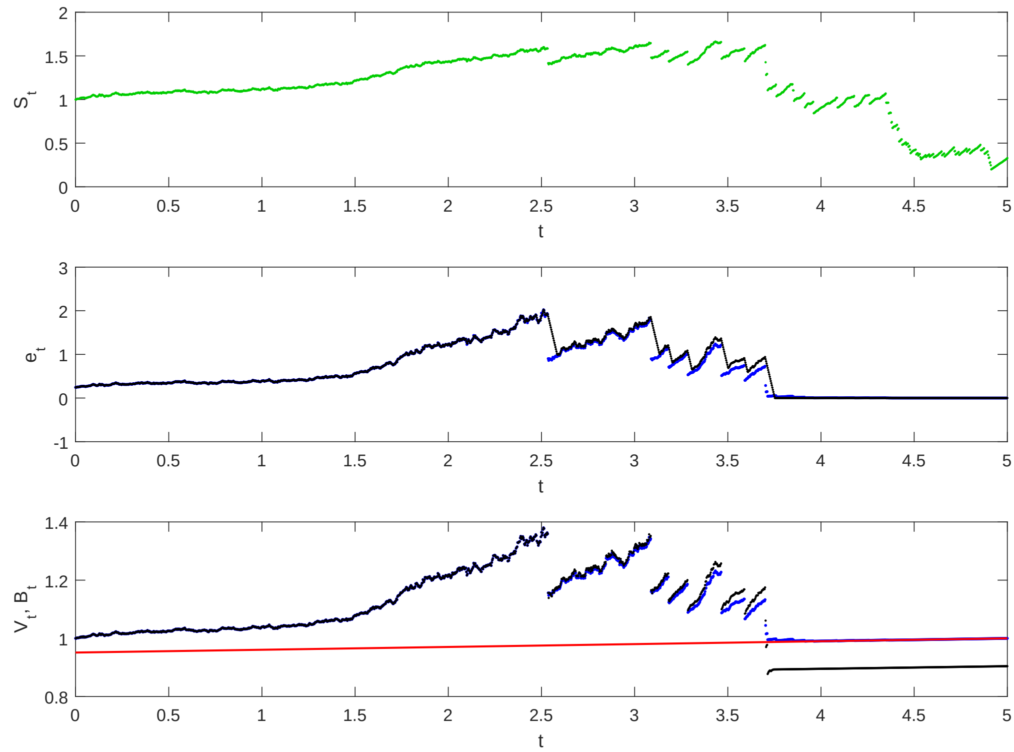

Figure 7: Sample paths of CPPI factors in the H-GJDM on January 5, 2015 with daily trading and liquidity constraint. *Top panel:* Asset price trajectory. *Middle panel:* Sample path of the risky exposure in the stylized daily trading (blue line) and in the liquidity constrained scenario of parameter $\Theta = 0.05$ (black line). *Bottom panel:* CPPI value in the stylized daily trading (blue line) and in the liquidity constrained scenario of parameter $\Theta = 0.05$ (black line), floor bond value (red line).

bearish or bullish markets but has potential of rewards in volatile markets that are expected to invert their trend over short periods of time.

This section is concerned with a simulation analysis along the lines of Section 5.2 for the measurement of the risk embedded in the implementation of the Constant-Mix strategy. We consider an analogous formal rebalancing calendar according to which the portfolio composition is re-evaluated at different equidistant time nodes which might be located at regular intervals of one day, one month, and one quarter, respectively. Following standard terminology in risk management, we define the loss of a strategy with time-horizon T as

$$L_T = -\left(V_T - V_0\, e^{r\,T}\right)\,,$$

where V_T and V_0 denote the value of the strategy at maturity and at the outset, respectively. Table 6 reports different measures of the loss of a Constant-Mix strategy with $m = 0.6$, under both the Hawkes-driven model (19) and its fixed intensity counterpart, and for different rebalancing frequencies. Inspection of the values of the 99% VaR and of the 99% ES reveals that in almost all cases the

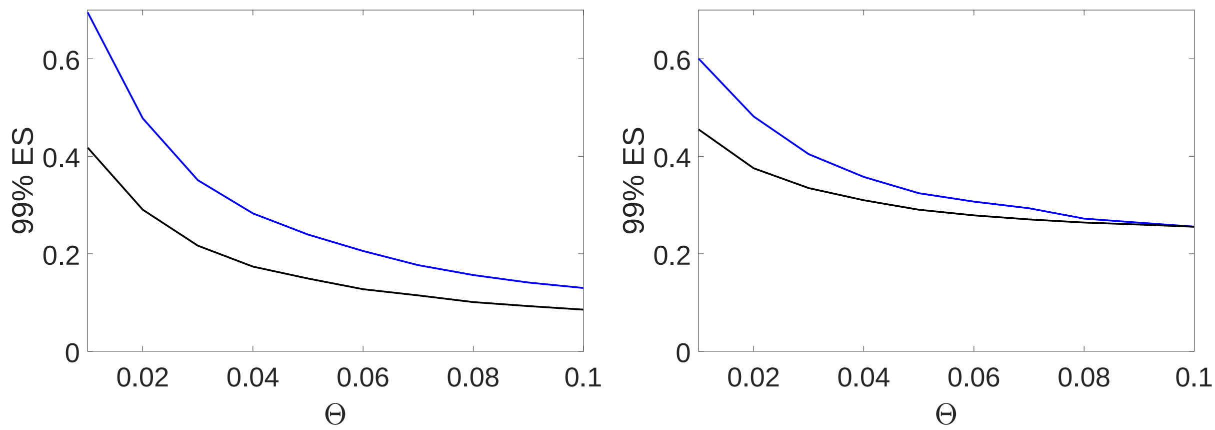

Figure 8: *Left panel:* Expected Shortfall at 99% level of the CPPI loss as function of the liquidity parameter Θ in the H-GJDM (blue line) and in the CP-GJDM (black line) on January, 5 2015. *Right panel:* Expected Shortfall at 99% level of the CPPI loss as function of the liquidity parameter Θ in the H-NGJDM (blue line) and in the CP-NGJDM (black line) on January, 5 2015.

Hawkes-driven model predicts a significantly higher portfolio loss compared to the one expected by the fixed intensity model. Surprisingly, overall the magnitude of the risk measures tends to remain unvaried irrespective of the different frequency settings for both jump size specifications.

Moreover, comparing the risk measures in Table 6 with those of the CPPI reported in Tables 2 and 3, we observe that on several of the crisis dates and for the low rebalancing frequencies, the CPPI leads to significantly higher risk measures. We stress the importance of this result as the CPPI is often perceived as being a trading strategy with low risk attached to it due to the embedded strategy floor. The CPPI performs poorly in scenarios where the risky asset increases to a high level before being hit by large negative shocks. In these scenarios the exposure to the risky asset can increase to more than the portfolio value due to the multiplier m. Under non-continuous trading, the shocks to the risky asset might incur before the CPPI manager has time to sell off the risky asset ultimately resulting in losses to the strategy above the initial investment. In particular, the risk measures for December 5, 2008 and April 3, 2009 in the Tables 2, 3, and 5 imply that losses of more than 100% occur with positive probabilities.

6 Conclusion

We study Constant Proportion Portfolio Insurance strategies in models allowing for self-excitement in the jump intensity of the risky asset. The probability of breaching the CPPI floor is derived in semi-closed form under the assumption of continuous-time trading. Moreover, we propose and detail how a measure change from the physical probability measure to a pricing measure can be performed. Additionally, we conduct a simulation experiment under a discrete-time rebalancing assumption and price the gap risk of the CPPI. We extend the analysis and compute various risk-measures under the physical probability measure, and find that failing to take the contagious nature of asset dynamics into account will tend to underestimate the risks involved in a CPPI strategy. Finally, we introduce illiquidity to the model by imposing an upper bound on the daily trading in the risky asset. The trading constraint has the implication that in scenarios where the risky asset underlying the CPPI grows to high levels followed by rapid negative shocks, the CPPI can incur heavy losses as the CPPI manager can not sell the risky exposure sufficiently before the CPPI floor is hit. The Hawkes-driven specifications are well-suited to capture this risk. Especially, for the less distressed dates we find that the fixed jump intensity specifications underestimate the risk measures compared to the contagion specifications.

Table 2: CPPI risk measures: Gaussian jump specification and equidistant rebalancing.

			Gaussian jumps							
			99% VaR		99% ES		Conditional expected loss		Probability of loss (%)	
			H-GJDM	CP-GJDM	H-GJDM	CP-GJDM	H-GJDM	CP-GJDM	H-GJDM	CP-GJDM
Pre-Crisis (2007)	Jan 05	d	0	0	4	0	20	160	0.21	0
		w	173	0	430	19	66	174	10.35	0.11
		2w	398	0	848	71	100	127	18.28	0.56
		m	871	71	1671	277	178	119	25.38	2.6
		3m	1976	390	3426	811	382	150	31.1	10.86
		4m	2306	511	3934	1021	453	169	31.11	13.64
	Apr 05	d	0	0	4	0	8	94	0.48	0
		w	84	0	258	15	47	66	7.48	0.22
		2w	295	0	662	50	89	65	14.01	0.77
		m	725	43	1391	167	163	77	22.52	2.44
		3m	1733	273	2998	616	356	129	29.13	8.43
		4m	1999	385	3413	795	420	149	29.21	10.89
	Jul 06	d	0	0	1	0	7	38	0.08	0
		w	13	0	79	1	23	45	3.6	0.03
		2w	92	0	258	8	41	58	9.1	0.13
		m	334	0	707	57	83	80	18.39	0.7
		3m	1156	154	2050	390	221	114	30.56	4.96
		4m	1444	235	2499	537	277	131	32.13	6.89
	Oct 05	d	43	20	209	199	34	109	6.9	1.87
		w	335	196	739	506	62	100	24.48	7.6
		2w	581	334	1162	746	91	110	32.51	12.75
		m	1091	589	1983	1156	156	134	40.7	20.84
		3m	2375	1256	3911	2172	344	218	46.8	32.79
		4m	2796	1494	4523	2528	418	254	46.69	35.13
Crisis (2008-2009)	Sep 05	d	0	0	2	1	2	24	1.18	0.04
		w	62	1	210	72	16	63	18.15	1.14
		2w	236	84	572	288	38	80	29.82	4.44
		m	726	394	1422	834	95	108	42.1	15.25
		3m	2339	1451	3819	2385	311	225	50.76	36.9
		4m	2956	1841	4709	2933	407	279	50.62	40.4
	Dec 05	d	157	274	375	560	16	28	48.88	41.48
		w	1226	1049	2304	1918	101	73	75.4	84.79
		2w	2323	1980	3911	3045	202	143	80.51	88.66
		m	4437	3436	6951	4965	413	296	82.49	92.23
		3m	9891	7415	14820	10763	1051	766	78.52	90.05
		4m	11755	8944	17385	13347	1296	965	76.11	88.28
	Apr 03	d	119	204	358	550	17	56	31.83	14.75
		w	629	698	1322	1331	60	75	57.13	46.13
		2w	1248	1255	2319	2092	118	114	65.26	62.61
		m	2537	2305	4171	3490	246	210	70.82	76.08
		3m	6001	5022	9041	7048	662	534	70.48	79.51
		4m	7273	6021	10781	8417	836	672	68.6	77.93
	Jun 04	d	48	60	182	227	11	51	21.39	5.28
		w	438	315	982	734	47	69	46.45	19.39
		2w	943	671	1833	1275	94	97	56.25	32.38
		m	2007	1341	3380	2228	201	153	63.66	50.86
		3m	4828	3112	7366	4562	552	353	65.26	65.11
		4m	5834	3767	8736	5389	698	440	63.77	65.4
Post-crisis (2015)	Jan 05	d	33	10	146	175	12	120	14.42	1.47
		w	356	246	740	569	48	103	38.27	9.32
		2w	606	403	1166	816	79	110	44.06	16.21
		m	1109	650	1989	1225	144	129	48.76	26.18
		3m	2408	1344	3966	2304	344	218	51.25	36.47
		4m	2837	1575	4611	2622	424	256	50.53	38.1
	Apr 02	d	0	0	9	1	2	45	4.14	0.03
		w	128	0	299	77	21	104	27.28	0.74
		2w	302	65	637	228	44	100	35.39	2.61
		m	730	216	1349	502	100	98	43.6	8.82
		3m	1954	680	3208	1291	290	160	48.9	21.18
		4m	2389	875	3826	1591	369	190	48.59	24.46
	Jul 02	d	2	0	32	18	8	47	4.1	0.37
		w	131	4	338	91	29	73	19.17	1.26
		2w	329	59	699	226	56	86	28.29	3.02
		m	772	209	1435	500	116	102	37.91	7.96
		3m	1972	677	3316	1286	308	163	44.78	20.59
		4m	2419	869	3942	1577	387	192	44.7	23.99
	Aug 05	d	0	0	1	0	4	3	0.19	0
		w	71	0	214	6	23	44	13.2	0.14
		2w	243	0	537	43	48	73	23.23	0.59
		m	677	67	1288	244	109	103	34.08	2.7
		3m	1959	436	3245	895	310	140	42.52	13.8
		4m	2387	592	3910	1149	391	165	42.59	17.09

The table reports the relative CPPI risk measures of H-GJDM and CP-GJDM for six different equidistant rebalancing rules: daily (d), weekly (w), fortnightly (2w), monthly (m), quarterly (3m), triannual (4m). We examine three market scenarios: the pre-crisis period (relative to the year 2007), the crisis (spanning from late 2008 to 2009), and the post-crisis period (referring to the year 2015). Value at Risk (VaR), expected shortfall (ES), and conditional expected loss are measured in basis points, while probability of loss is given in %. *Remark:* Number of simulations: 10^6.

Table 3: CPPI risk measures: Negative gamma jump specification and equidistant rebalancing.

			Negative gamma distributed jumps							
			99% VaR		99% ES		Conditional expected loss		Probability of loss (%)	
			H-NGJDM	CP-NGJDM	H-NGJDM	CP-NGJDM	H-NGJDM	CP-NGJDM	H-NGJDM	CP-NGJDM
Pre-crisis (2007)	Jan 05	d	504	480	1067	1062	150	209	14.31	9.20
		w	586	510	1204	1103	160	213	16.10	9.60
		2w	676	531	1347	1144	174	217	17.56	9.98
		m	862	597	1643	1244	207	227	19.82	10.89
		3m	1318	768	2364	1528	310	259	22.17	13.09
		4m	1468	831	2593	1624	354	274	21.99	13.67
	Apr 05	d	186	180	458	487	86	141	8.10	4.81
		w	262	210	590	542	93	146	11.11	5.40
		2w	342	242	731	599	105	152	13.61	6.04
		m	505	316	1003	727	133	164	17.45	7.38
		3m	963	528	1740	1068	231	201	22.12	10.98
		4m	1112	598	1944	1180	268	215	22.59	12.06
	Jul 06	d	1728	1774	3033	3160	336	409	27.72	21.90
		w	1763	1782	3088	3178	344	412	27.71	21.87
		2w	1784	1787	3140	3187	353	415	27.57	21.81
		m	1876	1816	3283	3222	375	422	27.45	21.83
		3m	2091	1854	3628	3281	444	444	26.09	21.40
		4m	2162	1860	3717	3272	472	451	25.23	21.10
	Oct 05	d	991	1135	1828	2060	148	208	35.6	28.56
		w	1131	1203	2064	2175	166	218	37.75	29.45
		2w	1279	1292	2279	2291	186	228	39.31	30.31
		m	1594	1450	2769	2535	231	251	41.65	32.25
		3m	2423	1893	4028	3176	372	320	43.21	35.28
		4m	2708	2046	4429	3399	430	349	42.58	35.68
Crisis (2008-2009)	Sep 05	d	0	0	25	23	12	65	2.09	0.36
		w	124	39	363	87	33	87	16.39	2.51
		2w	346	156	782	103	61	103	26.23	5.89
		m	894	480	1646	139	129	139	36.82	14.06
		3m	2562	1488	4050	262	375	262	43.50	30.62
		4m	3133	1867	4842	318	479	318	42.80	33.32
	Dec 05	d	693	915	1304	1610	55	63	69.14	80.44
		w	1915	1874	3286	2978	161	137	79.49	89.65
		2w	3037	2712	4941	4126	266	215	81.8	92.15
		m	5080	4210	7988	6154	478	371	82.35	92.96
		3m	10351	8240	15543	12549	1100	860	77.82	90.03
		4m	12039	9727	17887	15059	1331	1054	75.32	88.2
	Apr 03	d	536	624	1047	1179	44	54	65.29	58.39
		w	1881	1394	3200	2314	159	112	80.27	73.35
		2w	2988	1994	4815	3133	267	166	82.97	80.13
		m	5071	3085	7806	4595	482	275	83.56	84.87
		3m	10264	5878	15212	8343	1098	606	78.92	84.02
		4m	11857	6872	17406	9630	1321	739	76.45	82.35
	Jun 04	d	725	939	1406	1706	79	130	44.51	35.73
		w	1171	1228	2127	2130	121	155	53.16	42.19
		2w	1653	1536	2859	2540	170	183	56.98	47.43
		m	2594	2135	4191	3356	277	246	60.41	54.66
		3m	5037	3718	7600	5463	617	451	59.36	60.22
		4m	5937	4291	8791	6176	760	537	57.37	59.5
Post-crisis (2015)	Jan 05	d	1020	1225	1861	2189	140	234	40.5	27.3
		w	1181	1280	2121	2279	161	243	42.34	27.97
		2w	1352	1341	2382	2372	186	251	43.45	28.53
		m	1689	1486	2910	2569	240	271	44.76	29.89
		3m	2644	1824	4316	3059	414	331	43.86	32.13
		4m	2991	1940	4810	3245	487	356	42.56	32.37
	Apr 02	d	928	1055	1694	1957	131	231	37.77	22.46
		w	1092	1111	1943	2043	153	238	40.02	23.11
		2w	1255	1171	2200	2118	178	246	41.33	23.73
		m	1611	1275	2741	2279	237	263	42.80	25.11
		3m	2573	1585	4132	2749	421	318	41.62	27.45
		4m	2892	1690	4612	2909	496	340	40.14	27.89
	Jul 02	d	147	147	382	419	46	103	12.54	5.61
		w	353	219	767	553	67	115	23.64	7.43
		2w	561	296	1119	690	95	127	29.73	9.34
		m	987	460	1794	959	155	148	36.20	13.19
		3m	2095	915	3449	1674	342	212	40.51	21.60
		4m	2456	1071	3990	1906	417	236	40.04	23.70
	Aug 07	d	54	37	195	182	34	88	7.02	2.23
		w	228	90	533	294	51	100	18.98	3.58
		2w	408	150	845	411	75	111	25.83	5.08
		m	799	279	1474	645	130	131	33.41	8.27
		3m	1859	664	3081	1290	311	188	38.87	16.27
		4m	2192	803	3568	1497	382	211	38.62	18.52

The table reports the relative CPPI risk measures of H-NGJDM and CP-NGJDM for six different equidistant rebalancing rules: daily (d), weekly (w), fortnightly (2w), monthly (m), quarterly (3m), triannual (4m). We examine three market scenarios: the pre-crisis period (relative to the year 2007), the crisis (spanning from late 2008 to 2009), and the post-crisis period (referring to the year 2015). Value at Risk (VaR), expected shortfall (ES), and conditional expected loss are measured in basis points, while probability of loss is given in %. *Remark:* Number of simulations: 10^6.

Table 4: Gap risk fees, liquidity constrained scenario.

		GAP RISK FEE (%)			
		GAUSSIAN JUMPS		NEGATIVE GAMMA DISTRIBUTED JUMPS	
		H-GJDM	CP-GJDM	H-NGJDM	CP-NGJDM
PRE-CRISIS					
(2007)	Jan 05	0.06	0.01	0.19	0.24
	Apr 05	0.03	0	0.48	0.67
	Jul 06	0.01	0	0.72	1.01
	Oct 05	0.13	0.11	0.51	0.63
CRISIS					
(2008-2009)	Sep 05	0.03	0.04	0.01	0.01
	Dec 05	0.92	1.32	1.44	2.09
	Apr 03	0.34	0.67	1.65	1.38
	Jun 04	0.23	0.31	0.53	0.81
POST-CRISIS					
(2015)	Jan 05	0.13	0.14	0.53	0.69
	Apr 02	0.04	0.02	0.48	0.67
	Jul 02	0.05	0.02	0.14	0.10
	Aug 07	0.03	0.01	0.08	0.05

The table reports the CPPI upfront gap risk fee for the liquidity constrained scenario with parameter 0.05 under both the jump size specifications. We examine three market scenarios: the pre-crisis period (relative to the year 2007), the crisis (spanning from late 2008 to 2009), and the post-crisis period (referring to the year 2015). ARPEs on implied volatilities and gap risk fees are reported in percentage. *Remark:* Number of simulations: 10^6.

Table 5: CPPI risk measures, liquidity constrained scenario.

		GAUSSIAN JUMPS							
		99% VaR		99% ES		Conditional expected loss		Probability of loss (%)	
		H-GJDM	CP-GJDM	H-GJDM	CP-GJDM	H-GJDM	CP-GJDM	H-GJDM	CP-GJDM
PRE-CRISIS									
(2007)	Jan 05	537	0	1778	123	307	312	4.96	0.35
	Apr 05	268	0	1258	62	175	199	4.02	0.26
	Jul 06	0	0	450	16	211	213	1.30	0.06
	Oct 05	1030	517	2491	1326	202	249	14.93	6.51
CRISIS									
(2008-2009)	Sep 05	470	204	1716	949	163	223	4.98	2.55
	Dec 05	7725	6653	22545	18630	97	129	67.17	62.33
	Apr 03	3678	3857	9334	9450	82	177	44.92	34.51
	Jun 04	2696	1836	6268	3937	136	236	32.59	17.09
POST-CRISIS									
(2015)	Jan 05	951	619	2359	1471	134	281	22.76	7.12
	Apr 02	354	0	1304	374	128	307	8.23	1.07
	Jul 02	430	10	1475	401	138	225	8.30	1.5
	Aug 07	260	0	1214	106	216	240	3.30	0.34
		NEGATIVE GAMMA DISTRIBUTED JUMPS							
		99% VaR		99% ES		Conditional expected loss		Probability of loss (%)	
		H-NGJDM	CP-NGJDM	H-NGJDM	CP-NGJDM	H-NGJDM	CP-NGJDM	H-NGJDM	CP-NGJDM
PRE-CRISIS									
(2007)	Jan 05	758	571	1697	1289	161	202	17.49	10.80
	Apr 05	338	259	904	723	112	154	10.61	6.15
	Jul 06	1926	1887	3459	3393	320	383	29.90	23.82
	Oct 05	1637	1571	3247	2880	184	228	39.99	32.42
CRISIS									
(2008-2009)	Sep 05	754	383	2042	1202	102	190	8.15	4.05
	Dec 05	8526	8008	23259	22189	152	180	80.08	88.16
	Apr 03	8760	5180	23213	11985	210	213	79.05	71.38
	Jun 04	3239	2903	6741	5666	131	197	53.99	47.02
POST-CRISIS									
(2015)	Jan 05	1691	1611	3326	2934	172	250	44.6	30.71
	Apr 02	1534	1372	3015	2561	159	244	42.23	25.53
	Jul 02	783	381	1965	1045	117	159	18.94	8.32
	Aug 07	540	149	1491	614	111	154	12.46	3.97

The table reports the relative risk measures under the two model, H-JDM and CP-JDM, combined with the two jump specifications, for the liquidity constrained scenario with parameter 0.05. We examine three market scenarios: the pre-crisis period (relative to the year 2007), the crisis (spanning from late 2008 to 2009), and the post-crisis period (referring to the year 2015). Value at Risk (VaR), expected shortfall (ES), and conditional expected loss are measured in basis points, while probability of loss is given in %. *Remark:* Number of simulations: 10^6.

Table 6: Constant-Mix risk measures, equidistant rebalancing.

			GAUSSIAN JUMPS				NEGATIVE GAMMA DISTRIBUTED JUMPS			
			99% VaR		99% ES		99% VaR		99% ES	
			H-GJDM	CP-GJDM	H-GJDM	CP-GJDM	H-GJDM	CP-GJDM	H-GJDM	CP-GJDM
PRE-CRISIS (2007)	Jan 05	d	4474	2932	5452	3460	2040	2278	2978	2862
		m	4422	2930	5389	3455	2040	2278	2980	2861
		3m	4341	2928	5278	3446	2051	2279	2983	2857
	Apr 05	d	4205	2842	5164	3355	2539	2432	3485	2979
		m	4155	2840	5103	3351	2538	2430	3481	2976
		3m	4079	2837	4997	3343	2547	2430	3477	2971
	Jul 06	d	4258	2625	5221	3118	2277	2500	3260	3165
		m	4241	2623	5196	3115	2286	2501	3264	3163
		3m	4203	2620	5147	3107	2299	2503	3271	3161
	Oct 05	d	5692	3856	6677	4446	4874	3621	5920	4260
		m	5662	3851	6641	4439	4863	3619	5898	4255
		3m	5602	3841	6563	4424	4843	3611	5859	4242
CRISIS (2008-2009)	Sep 05	d	5334	3888	6472	4537	2317	3189	3587	3900
		m	5328	3884	6455	4530	2333	3186	3595	3894
		3m	5308	3875	6418	4513	2365	3185	3614	3885
	Dec 05	d	8508	6988	9229	7607	8461	7009	9184	7635
		m	8423	6969	9153	7584	8382	6991	9112	7612
		3m	8265	6932	9009	7536	8223	6952	8969	7566
	Apr 03	d	7708	5775	8646	6478	8286	6284	8999	6943
		m	7678	5764	8608	6461	8191	6273	8912	6924
		3m	7611	5737	8531	6429	8019	6245	8750	6887
	Jun 04	d	7419	5028	8385	5706	5002	4435	6338	5182
		m	7381	5019	8342	5693	5009	4432	6330	5172
		3m	7314	4999	8261	5668	5032	4415	6317	5153
POST-CRISIS (2015)	Jan 05	d	7226	3902	8194	4479	4285	3383	5586	4016
		m	7187	3894	8147	4471	4297	3377	5587	4016
		3m	7112	3883	8058	4456	4307	3372	5585	4016
	Apr 02	d	6831	3565	7881	4117	2973	3120	4288	3743
		m	6817	3559	7848	4111	2999	3115	4302	3739
		3m	6759	3554	7778	4097	3041	3111	4332	3731
	Jul 02	d	5833	3501	6920	4053	4302	3214	5476	3805
		m	5806	3496	6882	4047	4304	3211	5460	3800
		3m	5748	3489	6810	4033	4284	3207	5425	3789
	Aug 05	d	5261	3221	6369	3755	3608	2988	4734	3557
		m	5229	3219	6332	3749	3606	2987	4727	3553
		3m	5177	3211	6262	3738	3609	2982	4711	3544

The Table reports the Constant-Mix risk measures under the two models, H-JDM and CP-JDM, combined with the two jump specifications, and for three different equidistant rebalancing rules: daily (d), monthly (m), quarterly (3m). We examine three market scenarios: the pre-crisis period (relative to the year 2007), the crisis (spanning from late 2008 to 2009), and the post-crisis period (referring to the year 2015). The parameters of the Constant-Mix strategy are $m = 0.6$, $r = 0.01$, $q = 0$, $V_0 = 1$, and $T = 5$ years. Value at Risk (VaR) and expected shortfall (ES) are measured in basis points. *Remark:* Number of simulations: 10^6.

References

Aït-Sahalia, Y., Cacho-Diaz, J., and Laeven, R. J. (2015). Modeling financial contagion using mutually exciting jump processes. *Journal of Financial Economics*, 117(3):585–606.

Aït-Sahalia, Y. and Hurd, T. R. (2016). Portfolio choice in markets with contagion. *Journal of Financial Econometrics*, 14(1):1–28.

Ait-Sahalia, Y. and Jacod, J. (2009). Estimating the degree of activity of jumps in high frequency data. *Annals of Statistics*, 37(5A):2202–2244.

Aït-Sahalia, Y., Laeven, R. J., and Pelizzon, L. (2014). Mutual excitation in Eurozone sovereign CDS. *Journal of Econometrics*, 183(2):151–167.

Alfonsi, A. and Blanc, P. (2016). Dynamic optimal execution in a mixed-market-impact Hawkes price model. *Finance and Stochastics*, 20(1):183–218.

Andersen, T., Benzoni, L., and Lund, J. (2002). An empirical investigation of continuous-time equity return models. *Journal of Finance*, 57(3):1239–1284.

Bacry, E., Delattre, S., Hoffmann, M., and Muzy, J.-F. (2013). Modelling microstructure noise with mutually exciting point processes. *Quantitative Finance*, 13(1):65–77.

Balder, S., Brandl, M., and Mahayni, A. (2009). Effectiveness of CPPI strategies under discrete-time trading. *Journal of Economic Dynamics and Control*, 33(1):204–220.

Barndorff-Nielsen, O. and Shephard, N. (2006). Econometrics of testing for jumps in financial economics using bipower variation. *Journal of Financial Econometrics*, 4(1):1–30.

Boswijk, H. P., Laeven, R. J., and Lalu, A. (2015). Asset returns with self-exciting jumps: Option pricing and estimation with a continuum of moments. Technical report, working paper.

Bowsher, C. G. (2007). Modelling security market events in continuous time: Intensity based, multivariate point process models. *Journal of Econometrics*, 141(2):876–912.

Branger, N., Mahayni, A., and Schneider, J. C. (2010). On the optimal design of insurance contracts with guarantees. *Insurance: Mathematics and Economics*, 46(3):485–492.

Brémaud, P. (1981). *Point processes and queues.* Springer-Verlag, Halsted Press.

Brémaud, P. and Massoulié, L. (1996). Stability of nonlinear Hawkes processes. *The Annals of Probability*, 24(3):1563–1588.

Broadie, M., Chernov, M., and Johannes, M. (2007). Model specification and risk premia: Evidence from futures options. *Journal of Finance*, 62(3):1453–1490.

Carr, P. and Madan, D. B. (2005). A note on sufficient conditions for no arbitrage. *Finance Research Letters*, 2(3):125–130.

Chavez-Demoulin, V., Davison, A. C., and McNeil, A. J. (2005). Estimating value-at-risk: a point process approach. *Quantitative Finance*, 5(2):227–234.

Chavez-Demoulin, V. and McGill, J. (2012). High-frequency financial data modeling using Hawkes processes. *Journal of Banking & Finance*, 36(12):3415–3426.

Cont, R. and Tankov, P. (2009). Constant Proportion Portfolio Insurance in the presence of jumps in asset prices. *Mathematical Finance*, 19(3):379–401.

Dassios, A. and Zhao, H. (2011). A dynamic contagion process. *Advances in Applied Probability*, 43(3):814–846.

Dassios, A. and Zhao, H. (2012). Ruin by dynamic contagion claims. *Insurance: Mathematics and Economics*, 51(1):93–106.

Duffie, D., Pan, J., and Singleton, K. (2000). Transform analysis and asset pricing for affine jump-diffusions. *Econometrica*, 68(6):1343–1376.

Embrechts, P., Liniger, T., Lin, L., et al. (2011). Multivariate Hawkes processes: An application to financial data. *Journal of Applied Probability*, 48:367–378.

Eraker, B. (2004). Do stock prices and volatility jump? Reconciling evidence from spot and option prices. *Journal of Finance*, 59(3):1367–1403.

Errais, E., Giesecke, K., and Goldberg, L. (2010). Affine point processes and portfolio credit risk. *SIAM Journal on Financial Mathematics*, 1(1):642–665.

Hainaut, D. (2016). A model for interest rates with clustering effects. *Quantitative Finance*, 16(8):1203–1218.

Hawkes, A. (1971). Spectra of some self-exciting and mutually exciting point processes. *Biometrika*, 58(1):83–90.

Herrera, R. and Schipp, B. (2013). Value at risk forecasts by extreme value models in a conditional duration framework. *Journal of Empirical Finance*, 23:33–47.

Hirsa, A. (2009). Constant Proportion Portfolio Insurance. *Encyclopedia of Quantitative Finance*.

Jacod, J. and Shiryaev, A. (2003). *Limit Theorems for Stochastic Processes*. Springer: Berlin.

Jaisson, T., Rosenbaum, M., et al. (2015). Limit theorems for nearly unstable Hawkes processes. *The Annals of Applied Probability*, 25(2):600–631.

Jang, J. and Dassios, A. (2013). A bivariate shot noise self-exciting process for insurance. *Insurance: Mathematics and Economics*, 53(3):524–532.

Jessen, C. (2014). Constant Proportion Portfolio Insurance: Discrete-time trading and gap risk coverage. *The Journal of Derivatives*, 21(3):36–53.

Kallsen, J. (2006). A didactic note on affine stochastic volatility models. In *From Stochastic Calculus to Mathematical Finance*, pages 343–368. Springer.

Kallsen, J. and Muhle-Karbe, J. (2010). Exponentially affine martingales, affine measure changes and exponential moments of affine processes. *Stochastic Processes and their Applications*, 120(2):163–181.

Kokholm, T. (2016). Pricing and hedging of derivatives in contagious markets. *Journal of Banking and Finance*, 66:19–34.

Lewis, A. (2001). A simple option formula for general jump-diffusion and other exponential Lévy processes. *Envision Financial Systems and OptionCity.net.*

Nicolato, E. and Venardos, E. (2003). Option pricing in stochastic volatility models of the Ornstein-Uhlenbeck type. *Mathematical Finance*, 13(4):445–466.

Pan, J. (2002). The jump-risk premia implicit in options: Evidence from an integrated time-series study. *Journal of Financial Economics*, 63(1):3–50.

Pézier, J. and Scheller, J. (2013). Best portfolio insurance for long-term investment strategies in realistic conditions. *Insurance: Mathematics and Economics*, 52(2):263–274.

Protter, P. E. (2004). *Stochastic Integration and Differential Equations.* Springer-Verlag, second edition.

Stabile, G. and Torrisi, G. L. (2010). Risk processes with non-stationary Hawkes claims arrivals. *Methodology and Computing in Applied Probability*, 12(3):415–429.

Todorov, V. (2010). Variance risk-premium dynamics: The role of jumps. *Review of Financial Studies*, 23(1):345–383.

Weng, C. (2013). Constant Proportion Portfolio Insurance under a regime switching exponential Lévy Process. *Insurance: Mathematics and Economics*, 52(3):508–521.

A Appendix

A.1 Change of measure

We consider the structure-preserving change of measure from $\mathbb{P}$ to the pricing measure $\mathbb{Q}$ defined in (20). Combined with the assumption that the premium associated to jump risk stems entirely from the altered jump size distribution parameters, it can be explicitly expressed as

$$L_t = L_t^{(C)} L_t^{(J)} \tag{42}$$

with

$$\begin{aligned} L_t^{(C)} &= \mathcal{E}\left(-\xi\sigma W_t\right) \\ L_t^{(J)} &= \mathcal{E}\left(\sum_{j=1}^{H_t}\left(\kappa\left(Z_j\right)-1\right)-\int_{[-\infty,t]\times\mathbb{R}}\left(\kappa(z)-1\right)\nu^X(\omega;ds,dz)\right), \end{aligned}$$

where $\kappa(z) = \frac{\tilde{f}(z)}{f(z)}\mathbb{1}_{\mathrm{supp} f}(z)$, and $\nu^X(\omega;dt,dz) = \lambda_t f(z)dz\,dt$. We perform the change of measure through L on the log-price $X = \log(S)$ whose dynamics is given by

$$dX_t = \left[r - q - \frac{1}{2}\sigma^2 + \gamma_t + \left(\mu^X - \mu\right)\lambda_t\right]dt + \sigma\, dW_t + dJ_t - \mu^X \lambda_t dt\,,$$

where $J_t = \sum_{j=1}^{H_t} Z_j$, $\mu = \mathbb{E}\left[e^{Z_1}-1\right]$, and $\mu^X = \mathbb{E}[Z_1]$. By Girsanov's theorem we infer that $\tilde{W}_t := W_t + \xi\sigma t$ is a $\mathbb{Q}$–Brownian motion, the $\mathbb{Q}$-drift coefficient is given by

$$\tilde{b}_t = \left(r - q - \frac{1}{2}\sigma^2 + \gamma_t + \left(\mu^X - \mu\right)\lambda_t\right) - \xi\sigma^2 + \lambda_t\left(\tilde{\mu}^X - \mu^X\right),$$

where $\tilde{\mu}^X = \mathbb{E}^{\mathbb{Q}}\left[\tilde{Z}_1\right]$, and the $\mathbb{Q}$-compensator becomes $\tilde{\nu}^X(\omega;dt,dz) = \kappa(z)\,\nu^X(\omega;dt,dz)$ (cf. Jacod and Shiryaev (2003), Theorem III.3.24, or Kallsen (2006), Proposition 2.6). Due to the particular form of $\tilde{\nu}^X$, in view of the marked Hawkes characterization Proposition 2.2, the risk-neutral jump term is still a marked Hawkes process with $\mathcal{F}_t$–intensity λ_t. The risk-neutral dynamics of the stock price process $S = \exp(X)$ is easily obtained by the general Itô's formula and is given by

$$\frac{dS_t}{S_{t-}} = \left[r - q + \gamma_t - \xi\sigma^2 + \left(\tilde{\mu} - \mu\right)\lambda_t\right]dt + \sigma\, dW_t + dJ_t^S - \tilde{\mu}\lambda_t\, dt\,,$$

where $\tilde{\mu} = \mathbb{E}^{\mathbb{Q}}\left[e^{\tilde{Z}_1}-1\right]$.

The specific choice for the density process driving the change of measure outlined in (42) inherently leaves the jumping times, or equivalently the intensity process, unchanged. In the level-effect enriched intensity specification (8) the change of measure applies a reshape of the jump size distribution parameters and, when passing from $\mathbb{P}$ to $\mathbb{Q}$, to preserve the same jump intensity in terms of the "new" jumps it is necessary to put some restrictions on the risk-neutral jump size distribution parameters. Here we assume that the risk-neutral jump sizes $\left(\tilde{Z}_j\right)_{j\in\mathbb{N}}$ are linearly related to $\left(Z_j\right)_{j\in\mathbb{N}}$

through the parameter $\rho > 1$ as follows

$$\tilde{Z}_j = \rho\, Z_j \quad \forall\, j.$$

Accordingly, $\tilde{Z}_j \sim \text{NGam}\big(\kappa, \rho\theta\big)$, for any $j \geq 1$, and the dynamics of λ under $\mathbb{Q}$ is given by

$$d\lambda_t = \delta(\bar{\lambda} - \lambda_t)\, dt - \tilde{\epsilon}\, d\tilde{J}_t^{\lambda}\,,$$

where $\tilde{\epsilon} := \frac{\epsilon}{\rho}$ and $\tilde{J}_t^{\lambda} = \sum_{j=1}^{H_t} \tilde{Z}_j$.

Finally, in the Gaussian intensity framework, we assume $\tilde{\sigma_J} = \sigma_J$ to achieve identification of jumps in $\mathbb{Q}$ through the jump-risk premium.

A.2 Martingale property of the density process L_t

Define

$$M_t = [\,\lambda_t \quad \Xi_t\,]^{\top}\,,$$

λ_t being the intensity process under either jump specification, and Ξ_t being the process embedded in the change of measure with dynamics given by

$$d\Xi_t = -\xi\,\sigma\, dW_t + d\sum_{j=1}^{H_t}\big(\kappa(Z_j) - 1\big) - \mathbb{E}\,[\kappa(Z_1) - 1]\;\lambda_t\, dt.$$

Adopting the notation of Kallsen (2006), the process M is an $\mathbb{R}^2-$valued semimartingale with affine differential characteristics

$$\begin{aligned}
\beta\,(\mathrm{m}_1, \mathrm{m}_2) &= \beta_0 + \sum_{j=1}^{2} \mathrm{m}_j\, \beta_j \\
\gamma\,(\mathrm{m}_1, \mathrm{m}_2) &= \gamma_0 + \sum_{j=1}^{2} \mathrm{m}_j\, \gamma_j \\
\phi\,(\mathrm{m}_1, \mathrm{m}_2, B) &= \phi_0 + \sum_{j=1}^{2} \mathrm{m}_j\, \phi_j(B) \quad \text{ for } B \in \mathcal{B}(\mathbb{R}^2),
\end{aligned}$$

relative to admissible Lévy-Khintchine triplets $\big(\beta_j, \gamma_j, \phi_j\big)$, $j = 0, 1, 2$, of the form

$$\big(\beta_0, \gamma_0, \phi_0\big) = \left([\,\delta\,\bar{\lambda} \quad 0\,]^{\top}, \begin{bmatrix} 0 & 0 \\ 0 & \xi^2\,\sigma^2 \end{bmatrix}, 0 \right)$$

$$\big(\beta_1, \gamma_1, \phi_1(B)\big) = \begin{cases} \left([\,-\delta - \epsilon\mathbb{E}\,[Z_1] \quad 0\,]^{\top}, \begin{bmatrix} 0 & 0 \\ 0 & 0 \end{bmatrix}, \int \mathbb{1}_B\,(-\epsilon\, z, \kappa(z) - 1)\; f(z)\, dz \right), & \text{if } Z_j \sim \text{NGam}(\kappa, \theta) \\ \left([\,-\delta + \epsilon \quad 0\,]^{\top}, \begin{bmatrix} 0 & 0 \\ 0 & 0 \end{bmatrix}, \int \mathbb{1}_B\,(\epsilon, \kappa(z) - 1)\; f(z)\, dz \right), & \text{if } Z_j \sim \mathcal{N}(m_J, \sigma_J) \end{cases}$$

$$\big(\beta_2, \gamma_2, \phi_2\big) = \left([\,0 \quad 0\,]^{\top}, \begin{bmatrix} 0 & 0 \\ 0 & 0 \end{bmatrix}, 0 \right),$$

where $B \in \mathcal{B}(\mathbb{R}^2)$, and the identity $h(z) = z$ is used as truncation function. These triplets are admissible with $m = 1$. Furthermore, if the following conditions hold:

1. $\phi_j\left(\{z \in \mathbb{R} : \kappa(z) < 0\}\right) = 0, \quad \text{for } j = 0,1\,,$
2. $\displaystyle\int_{\{\kappa(z)-1>1\}} (\kappa(z) - 1)\, \phi_j(dz) < \infty, \quad \text{for } j = 0,1\,,$
3. $\beta_j^{(2)} = 0, \quad \text{for } j = 0,1,2\,,$
4. $\displaystyle\int_{\{\Delta\lambda>1\}} (\Delta\lambda)\, \kappa(z)\, \phi_j(dz) < \infty, \quad \text{for } j = 1\,,$

Corollary 3.9 in Kallsen and Muhle-Karbe (2010) yields that the process $L_t = \mathcal{E}(\Xi_t)$ is a martingale. Here, Condition 1 is evidently satisfied by construction for $j = 0$ and so is for $j = 1$ since κ is, by definition, a non-negative function. For $j = 0$, Condition 2 is also immediately verified by construction. When $j = 1$, regardless the jump size choice, the integral in Condition 2 is proved to be finite being the difference between the c.d.f. of Z and the c.d.f. of $\tilde{Z}$. In both the two jump specifications, the drift Condition 3 clearly holds by construction. As regards the final condition, for Gaussian jumps we obtain $\{\Delta\lambda > 1\} = \{\epsilon > 1\}$ and one sees immediately that the finiteness of the integral in Condition 4 is guaranteed as long as $\epsilon < \infty$. Finally, Condition 4 is fulfilled in the negative gamma jump specification as long as the mean of the jump sizes and ϵ are finite.

A.3 Martingale property of the discounted price process $e^{-(r-q)\,t} S_t$

Define

$$M_t = [\,\lambda_t \quad \tilde{X}_t\,]^\top,$$

λ_t being the intensity process under either jump specification, and $\tilde{X}_t$ being the discounted log price process with dynamics given by

$$d\tilde{X}_t = \left(-\frac{1}{2}\sigma^2 - \tilde{\mu}\,\lambda_t\right) dt + \sigma\, d\tilde{W}_t + d\sum_{j=1}^{H_t} \tilde{Z}_j.$$

Adopting the notation of Kallsen (2006), the process M is an affine process whose Lévy-Khintchine triplets $(\beta_j, \gamma_j, \phi_j)$, $j = 0,1,2$, meet the equations

$$(\beta_0, \gamma_0, \phi_0) = \left(\left[\delta\,\bar{\lambda} \quad -\frac{\sigma^2}{2}\right]^\top, \begin{bmatrix} 0 & 0 \\ 0 & \sigma^2 \end{bmatrix}, 0\right)$$

$$(\beta_1, \gamma_1, \phi_1(B)) = \begin{cases} \left(\left[-\delta - \epsilon\,\mathbb{E}^{\mathbb{Q}}[\tilde{Z}_1] \quad -\tilde{\mu} + \mathbb{E}^{\mathbb{Q}}[\tilde{Z}_1]\right]^\top, \begin{bmatrix} 0 & 0 \\ 0 & 0 \end{bmatrix}, \int \mathbb{1}_B(-\epsilon\, z, z)\, \tilde{f}(z)\, dz\right), & \text{if } \tilde{Z}_j \sim \text{NGam}(\kappa, \rho\theta) \\ \left(\left[-\delta + \epsilon \quad -\tilde{\mu} + \mathbb{E}^{\mathbb{Q}}[\tilde{Z}_1]\right]^\top, \begin{bmatrix} 0 & 0 \\ 0 & 0 \end{bmatrix}, \int \mathbb{1}_B(\epsilon, z)\, \tilde{f}(z)\, dz\right), & \text{if } \tilde{Z}_j \sim \mathcal{N}(\tilde{m}_J, \sigma_J) \end{cases}$$

$$(\beta_2, \gamma_2, \phi_2) = \left([0 \quad 0]^\top, \begin{bmatrix} 0 & 0 \\ 0 & 0 \end{bmatrix}, 0\right),$$

where $B \in \mathcal{B}(\mathbb{R}^2)$, and the identity $h(z) = z$ is used as truncation function. These triplets are admissible with $m = 1$. Furthermore, if the following conditions hold:

1. $\mathbb{E}\left[e^{M_0^{(2)}}\right] < \infty$
2. $\int_{\{z>1\}} e^z \phi_j(dz) < \infty, \quad \text{for } j = 0, 1$
3. $\beta_j^{(2)} + \frac{1}{2}\gamma_j^{(2,2)} + \int \left(e^z - 1 - z\right) \phi_j(dz) = 0, \quad \text{for } j = 0, 1, 2$
4. $\int_{\{\Delta\lambda>1\}} (\Delta\lambda)\ e^z \phi_j(dz) < \infty, \quad \text{for } j = 1$

the time-homogeneous counterpart of Corollary 3.4 in Kallsen and Muhle-Karbe (2010) yields that the process $\tilde{S}_t = e^{\tilde{X}_t}$ is a martingale. Here, Condition 1 clearly holds since $\mathbb{E}\left[e^{M_0^{(2)}}\right] = \mathbb{E}\left[e^{\tilde{X}_0}\right] = \tilde{S}_0 < \infty$. Condition 2 is evidently satisfied by construction for $j = 0$, and for $j = 1$ we consider the two jump specifications separately. For negative gamma jump distribution having support in $(-\infty, 0]$ it is easily seen that the integral in Condition 2 has the value zero. In the Gaussian case, it is easy to check that

$$\int_{\{z>1\}} e^z \tilde{f}(z)\, dz = e^{\tilde{m}_J + \frac{\sigma_J^2}{2}} \left(1 - F^{\mathcal{N}_{0,1}}\left(\frac{\tilde{m}_J - \sigma_J^2 + 1}{\sigma}\right)\right),$$

where $F^{\mathcal{N}_{0,1}}$ denotes the c.d.f. of a standard normally distributed r.v., hence the finiteness of the integral is guaranteed as long as the mean and the standard deviation of the jump sizes are finite. Condition 3, regarding the drift, is easily fulfilled by construction. As regards the final condition, for Gaussian jumps an easy computation shows that the integral in Condition 4 is finite as long as ϵ, the mean and the standard deviation of the jump sizes are finite. The same conclusion can be drawn for the case of negative gamma distributed jumps where it can be easily checked that Condition 4 holds as long as the mean of the jump sizes and ϵ are finite.